Changes in Ecosystem Functioning Along a Eutrophication Gradient in Waihī Estuary

A thesis

submitted in partial fulfilment

of the requirements for the degree

of

Master of Environmental Science (Research)

at

The University of Waikato

by

KIT SQUIRES

THE UNIVERSITY OF
WAIKATO
Te Whare Wānanga o Waikato

2019

Abstract

Soft-sediment coastal ecosystems are important sites for a multitude of ecosystem functions, including primary production, organic matter recycling and nutrient processing. Intertidal areas host an array of fauna and flora that can alter pathways and processes which underpin function, support higher food webs and ecosystem services. Anthropogenic impacts on coastal areas are increasing in frequency and intensity. One of the key pressures to New Zealand estuaries, and globally, is that of increased run-off from land. This can cause eutrophication, which is the ecological response to increased nutrients. Waihī Estuary, in Bay of Plenty, New Zealand, has been influenced by farming intensity, coastal development, and stream channelising, which has increased sediment and nutrient inputs recently and over the past 90 years; resulting in frequent algal blooms. This thesis explores the effect eutrophication is having on ecosystem functioning along a gradient of change.

Field sampling was carried out over summer 2018 and used space as a proxy for time, sampling seven sites over a naturally occurring eutrophication gradient. Solute exchanges (O_2, NH_4^+-N, PO_4^{3-}-P, NO_x-N), were measured using benthic flux chambers over one tidal period. At each site, environmental variables and the macrofaunal community were also quantified. Biotic and abiotic drivers of function were examined firstly on a site by site basis, to gain resolution of fine scale flux dynamics. Non-metric distance based linear models were then created to evaluate changes in function across the spectrum of sites using sequential tests where organic matter content was fitted first.

Results from this study indicate increasing organic matter content was a major contributing factor to ecological shifts, cascading biotic and abiotic interactions, and feedback loops. Increasing organic matter content increased sediment oxygen demand to the point of hypoxia (and potentially anoxia), particularly where algal mats (*Gracilaria* spp.) were present. *Gracilaria* spp. seemingly capped the sediment, prevented light penetration and significantly influenced sediment oxygen consumption. Photosynthetic efficiency ($GPP_{chl\ a}$) also decreased with organic matter enrichment. In association with increased sediment oxygen consumption, NH_4^+-N and PO_4^{3-}-P showed a 2.6 and 2-fold increase in efflux (respectively) under dark conditions. Redox pathways were altered as eutrophication increased and,

where oxygen was depleted, NO_x-N was taken up by sediments and utilised as an electron acceptor.

Organisms responded positively to organic enrichment to a point, but once this threshold was exceeded, taxonomic richness and individual abundance reduced. Although sediment variables explained the greatest proportion of variance in flux models across the gradient, key bioturbating species had disproportionate effects on solute exchanges. These organisms were sensitive to changes in sediment conditions. The New Zealand cockle *Austrovenus stutchburyi* and tellinid bivalve *Macomona liliana* were the first species to decline in response to eutrophication. *A. stutchburyi* increased NH_4^+-N efflux, but declined in number with eutrophication, which simultaneously increased NH_4^+-N efflux. A burrow building polychaete, *Ceratonereis* spp. enhanced NO_x-N uptake to sediments indicating nitrification-denitrification coupling. However the opportunistic amphipod *Paracorophium* spp. dominated site 4, where increased NO_x-N efflux (though continuous burrow ventilation) indicated a potentially important species for ammonification and subsequent nitrification.

This study demonstrates how changes in ecosystem functioning due to eutrophication can result in undesirable shifts within estuarine systems. These changes are often difficult to remediate and can impede the services that estuaries provide.

Acknowledgements

I am in constant awe at the number of people who have invested time into helping me progress with my MSc journey. While acknowledgements may seem like superficial words, I, from the depth of my heart, am truly thankful for all who helped. First and foremost, I would like to thank my chief supervisor, Hazel Needham. Your elite level of dedication, interest, knowledge, and encouragement is extremely valued, I could not have asked for a more supportive supervisor. Thank you for the countless meetings, your willingness to give time, and invaluable direction in the field and through every other aspect of my MSc. To my secondary supervisor, Drew Lohrer, thank you for your knowledge and guidance with statistics, writing, lending field equipment, and allowing me to ID at NIWA. Your input is greatly appreciated, and I hope that one day, we will both be playing drums on the same stage – rock on.

I would like to thank the University of Waikato Strategic Investment Fund, for financing this project and ultimately making all this possible. Thank you to Te Arawa ki Tai charitable trust, particularly Raewyn Bennet who organised meeting with local Iwi members prior to my work in Waihī Estuary, and to Chris Battershill for making these introductions. Thank you to Te Arawa Lakes trust for allowing access through their land, and to Elaine Tapsell for facilitating this. To the residents of Little Waihī who made fieldwork pleasurable through providing food and history of the area, thank you for being so welcoming.

To everyone who helped with the long fieldwork days; Tarn Drylie, Georgina Flowers, Rebecca Gladstone-Gallagher, Steph Mangan and Vera Rullens; thank you for your time, effort, and for making the fieldwork a great experience. A massive thank you to Barry Greenfield and Sarah Hailes for teaching me how to identify macrofauna, and to Grady Petersen for checking my sorting. Thanks to those who helped with sediment analyses; Adrienne Gooden, Annette Rodgers and Janine Ryburn. Thank you to Dana Clark, Emily Douglas and Joanne Ellis for teaching me how to run DistLM's and giving me advice on statistics. To those who proof read my thesis; Uncle Ross Barker, Brieana Booth, Nicole Hanrahan, Daniel Squires; thank you very much. Major thank you to Cheryl Ward for helping compile and format my thesis.

I would like to take this space to thank family and friends, in particular my mum and dad, who loved, supported, and cheered me along the way. Though it may be hard to understand what I do, you are all proud of me nonetheless and for that, I am deeply grateful. To my girlfriend Nicole, for your encouragement, camaraderie, doing your MSc alongside me, and ensuring I finished well; words cannot describe my admiration for you. To my office buddies Bridgette Farnworth and Vera Rullens, thank you for answering many questions and looking out for me along the way. Thank you to fellow master students; Kate, Kelly, Lolita, and Nicole, UOW staff and NIWA staff for providing quality banter and encouragement during tea and lunch breaks, these times created memories that hold much joy.

Overall, I hold much gratitude to everyone who was involved in my life while I embarked on this journey of discovery, purpose and upskilling. Whether big or small, your input was greatly valued and it would not have been nearly as good to do this without you. One quote to summarise my masters and to give motivation to those seeking to do the same, as the great nineteenth-century German philosopher Friedrich Nietzsche wrote:

"He whose life has a why can bear almost any how."

Table of Contents

List of Figures

List of Tables

Chapter One

Introduction

Marine soft sediment ecosystems are one of the most common environments on Earth, and include large expanses of intertidal area. Hosting an array of organisms, estuaries are an intertidal buffer between the land, rivers and the open coast. These highly productive ecosystems provide an array of important ecosystem functions that significantly contribute to the services estuaries provide (Barbier *et al.*, 2011). Such services include fisheries, decontamination, protection from storm waves and recreation, as well as cultural services (Barbier *et al.*, 2011; Barbier, 2016). New Zealand estuaries provide kai moana (sea food) collection sites for Māori who have strong associations with the whenua (land). Therefore a degradation in the whenua can result in a degradation of Māori core beliefs (Marsden & Adkins, 2010).

The functions that underpin the services humankind values are driven by the organism-sediment dynamics of benthic systems (Welsh, 2003; Hattam *et al.*, 2015). Estuarine benthic fauna have significant influence on primary and secondary production, regulating phytoplankton biomass (and hence, turbidity), nutrient cycling, as well as providing a food source for higher trophic levels (Underwood & Kromkamp, 1999; Cloern, 2001; Lohrer *et al.*, 2010). A lot of the above process occur at the sediment-water interface, which is modified and extended through the lateral and vertical movement of macrofauna as they bioturbate the upper layers of sediment (Kristensen, 2000; Shull *et al.*, 2009; Crawshaw *et al.*, 2019). This increases the area available for oxidative exchange, and in turn, influences the fluxes of nutrients to and from the sediment (Kristensen, 2000; Lohrer *et al.*, 2004; Thrush *et al.*, 2006).

Anthropogenic impacts on estuarine environments are growing exponentially (Rabalais *et al.*, 2014; Fuller *et al.*, 2015). Humankind has a reliance on coastal services, but are also impacting the processes that deliver them (O'Meara *et al.*, 2017). Such processes are affected by the non-linear accumulation of multiple stressors that flow through networks of ecosystem functions, working in a conjunctional rather than individual nature (Adams, 2005; Thrush *et al.*, 2008; Lohrer *et al.*, 2011; O'Meara *et al.*, 2017). Attempting to tease apart these

interactions comes with inherent difficulty due to their complexity, non-linearity and both positive and negative feedback loops that change under certain environmental conditions. Possibly one of the most pressing multi-stressors to consider however, is the overloading of nutrients to receiving environments.

Over the past 150 years there has been a 10 fold increase in reactive nitrogen use, with anthropogenic activities (primarily farming intensification), accounting for more than twice the amount of reactive nitrogen (N) utilisation when compared to naturally occurring processes (Galloway *et al.*, 2004; 2008). This increases the potential for the mobilisation of N into rivers, which are now transporting up to six times more inorganic N than prior to the industrial revolution (Galloway & Cowling, 2002). All rivers eventually lead to marine receiving environments, where the net accumulation of N can have (and has had) negative impacts on marine systems (Bricker *et al.*, 2008; Tay *et al.*, 2013; Thrush *et al.*, 2017). Estuarine environments are particularly susceptible to nutrient enrichment as they are partially enclosed shallow bodies of water that are highly productive (Potter *et al.*, 2010). While N is not the only stressor to intertidal areas, it is amongst the greatest influences of globally accelerated anthropic change (Vitousek *et al.*, 1997; Boesch, 2002).

1.1 Eutrophication

Defined by Nixon (1995) as the ecological response to an increased supply of organic matter and rate of primary production, eutrophication typically is the process of elevated nutrient addition, generally resulting in undesirable ecosystem changes. Eutrophication is often seen through increased algal blooms, an altered sediment environment and a decrease in the abundance and diversity of the benthic community (Hale *et al.*, 2016; Douglas *et al.*, 2018). In healthy estuarine systems both N and phosphorous (P) can be considered as limiting nutrients for plant growth (Conley *et al.*, 2009b), varying spatially and seasonally. Areas where fresh and salt water mix tend be P limited, and summer months are associated with N limitation, while months leading up to summer are generally P limited (Conley, 1999; Blomqvist *et al.*, 2004).

Positive aspects of nutrient inputs are seen by an increase in the rate of primary production, which has cascading bottom-up effects on the food chain (Paerl, 2006).

On the other hand, while systems can thrive with appropriate nutrient levels, there is a point whereby nutrients exceed the system's capacity to process them, resulting in increased water column production (Rabalais *et al.*, 2009). The build-up of algae has negative implications for ecosystem functioning and services, as blooms shade photosynthetic organisms (influencing MPB production) and alter biogeochemical pathways (Nelson *et al.*, 2015). Subsequent algal bloom degradation can cause hypoxia (the biotic deficiency of oxygen) and ultimately anoxia (the absence of oxygen) which can change the redox pathway in the sediments and lead to hydrogen sulphide production (Bohorquez *et al.*, 2013; Lyons *et al.*, 2014; Nelson *et al.*, 2015). Other processes that can cause eutrophication include – but are not limited to – changes in biological interactions (i.e. reduced grazing pressure) and system characteristics (stratification and circulation) (Rabalais *et al.*, 2009; Cosme & Hauschild, 2017) However, causes of eutrophication should not be thought of as eutrophication itself (Rabalais *et al.*, 2009).

The above processes can result in benthic fauna migration or mortality (Levin *et al.*, 2009). When oxygen is lost, and sulphides are produced, the redox potential discontinuity layer (RPD; the transitional zone between oxic and anoxic sediment) is compressed closer to the sediment surface. The seminal work by Pearson and Rosenberg (1978) showed that species diversity and individual abundance increases with initial organic matter enrichment, followed by a decline in diversity, where few opportunistic species then become incredibly abundant. As organic content continues to increase, the opportunistic species rapidly decline, and species mortality becomes more pronounced. However, organic matter is not the only factor that can impact benthic communities and tends to be correlated with other stressors.

1.1.1 Multiple stressors

While excess N and P are the main drivers of eutrophication, they are far from the only drivers acting as stressors on intertidal benthic ecosystems. Using the definition that a stressor is any factor that adversely affects the fitness of individual organisms (Thrush *et al.*, 2008), then species abundance and metabolic efficiency may simultaneously be affected by multiple natural and/or anthropic stressors (Thrush *et al.*, 2008). Nutrients, pollutants, sedimentation, hypoxia, and alterations

in hydrology and habitat are some stressors that can influence the capability of benthic organisms to function as an effective community (Adams, 2005). Such stressors can have direct effects on resident biota (Fleeger *et al.*, 2003), but multiples stressors do not always behave in a cumulative manner; instead occurring concurrently to increase or dampen stressor impacts (Ellis *et al.*, 2015). Thus direct effects of multiple stressors have the potential to impact broad ecosystem functions.

Another dominant stressors in New Zealand estuaries is the alteration of sediment grain size through the process of sedimentation (Thrush *et al.*, 2004). The export of terrestrially derived sediment to the ocean has long been considered, and still remains a natural process. However, in recent years it has been noted by Valiela *et al.* (2014); Fuller *et al.* (2015) that soil erosion from anthropogenic land use change (e.g. construction of roads, buildings; and livestock farming and logging practices) within coastal catchments increases terrestrial sediment loading to receiving environments. Hence, terrigenous sediment is considered a disturbance to nearshore marine and estuarine environments (Lohrer et al., 2006). Deposits of fine silts and clays further alter grain size distribution and ecosystem function through the clogging of pore space, and when suspended in the water column, accounts for 80% of light variability (Pratt *et al.*, 2014a; Pratt *et al.*, 2014b). With eutrophication, these stressors are interlinked, where for example, increased fine sediments are generally highly correlated with organic matter input (De Falco *et al.*, 2004; Douglas *et al.*, 2018). High organic matter is often associated with increased algal blooms, which then have the potential to cause localised hypoxia (Nelson *et al.*, 2015).

1.1.2 Hypoxia

Hypoxia is the state of having insufficient dissolved oxygen (herein DO). The underlying processes behind natural and/or anthropic hypoxia entail the biological oxygen demand exceeding the molecular oxygen diffusion from surface waters (Levin *et al.*, 2009). This process is generally attributable to an increased rate of microbial respiration, which is fuelled by the systems incapacity to utilise elevated photosynthetic carbon production driven by nutrient enrichment (Rabalais *et al.*, 2010). However, defining the point at which hypoxia occurs has proven difficult. Vaquer-Sunyer and Duarte (2008) argue that the 55% of reports (see Vaquer-

Sunyer & Duarte, 2008, Table S2 in Supporting Information) defining hypoxia as 2 mg L^{-1} or approximately 30% DO saturation, are underestimating hypoxia onset for a large proportion of organisms. Furthermore, organisms show variable tolerances to hypoxia, both physiologically and behaviourally (Gray *et al.*, 2002), meaning the definition of hypoxia is less of a conventional oxygen threshold, and more of a realisation of the system being examined (Farrell *et al.*, 2009).

Literature is limited on how the effects of multiple stressors, as a result of eutrophication, interact to influence the function of estuarine systems. Recent studies by O'Meara *et al.* (2017); Thrush *et al.* (2017); Douglas *et al.* (2018), amongst others, point toward measuring changes in community structure associated with multiple stressors through calculating nutrient exchange at the sediment-water interface. Benthic flux (the exchange of nutrients to and from the sea floor) is governed by detrital sedimentation, subsequent decomposition, and the reciprocal to and from transportation of nutrients between the sediment and overlying waters via diffusion/advection, faunal activity and the microbial community (Herbert, 1999). Within sediment is an array of nutrient transformations that take place under differing sediment and biological conditions.

1.2 Nutrient cycling

1.2.1 Nitrogen

Nutrient cycling in shallow water estuarine environments is a complex process, as many different physical, chemical and biological factors interact. Figure 1.1 shows that N is subject to a number of multi-directional oxidation and reduction transformations, including ammonification, nitrification, nitrate reduction, denitrification, and anammox (anaerobic ammonium oxidisation) (Blackburn, 1986). Particulate organic nitrogen (PON) settles onto sediments from the overlying water column, and ammonia is released via a process termed ammonification (Herbert, 1999). The quality and quantity of PON determines if ammonification follows a relatively simple deamination reaction, or a sequence of complex metabolic pathways (Herbert, 1999). If the latter occurs, then ammonification metabolic pathways will include hydrolytic enzymes that break down nitrogen-containing polymers to sub-units of soluble monomers; making ammonium available for nitrification (Herbert, 1999). Nitrification is a process that

requires oxygen, and as such, occurs in oxic sediment where oxygen readily diffuses to and from the water column (Figure 1.1). Before fixed N can be removed (via denitrification or anammox), N must be converted to nitrite (NO_2^-) or nitrate (NO_3^-). Nitrification is mediated by ammonia-oxidising bacteria (NH_4^+) to NO_2^-), and is then further oxidised to NO_3^- by nitrate-oxidising bacteria (Henriksen & Kemp, 1988). When nitrite and nitrate are buried into anoxic sediment through high organic loading and/or high sulphide oxidation rates, dissimilatory nitrate reduction to ammonium (DNRA) can occur (Burgin & Hamilton, 2007).

DNRA microbially reduces NO_3^- to NO_2^-, which is then oxidised to NH_4^+ (Dalsgaard *et al.*, 2005; Jäntti *et al.*, 2011). However, this can be considered a harmful processes in terms of eutrophication, because compared to nitrate, ammonium is more bioavailable (Burgin & Hamilton, 2007).

1.2.2 Denitrification pathways

Once ammonium is available in anoxic sediments, the bacterially mediated process of anammox can occur, where ammonium and nitrite are used to form nitrogen gas (Burgin & Hamilton, 2007). The anammox pathway of N removal remains relatively unknown, and other processes such as denitrification tend to be of greater significance in marine systems, are quantified more frequently, and better understood (Burgin & Hamilton, 2007). Denitrification is important to remove nitrogen from estuarine and aquatic ecosystems, through regulating the quantity of N to primary producers, therefore providing a buffer against a eutrophic state (Falkowski *et al.*, 1998; Teixeira *et al.*, 2010). Denitrification is the process of bioavailable, electron accepting nitrogen compounds (NO_3^- and NO_2^-) being anaerobically converted via heterotrophic bacteria to nitrogenous gasses (nitrous oxide; N_2O and nitrogen gas; N_2) (Teixeira *et al.*, 2010). These gases are then released into the atmosphere. The removal of nitrogen through denitrification in estuaries accounts for 10 to 80%, thereby one of the greatest mechanisms of nitrogen removal from these systems (Nixon *et al.*, 1996).

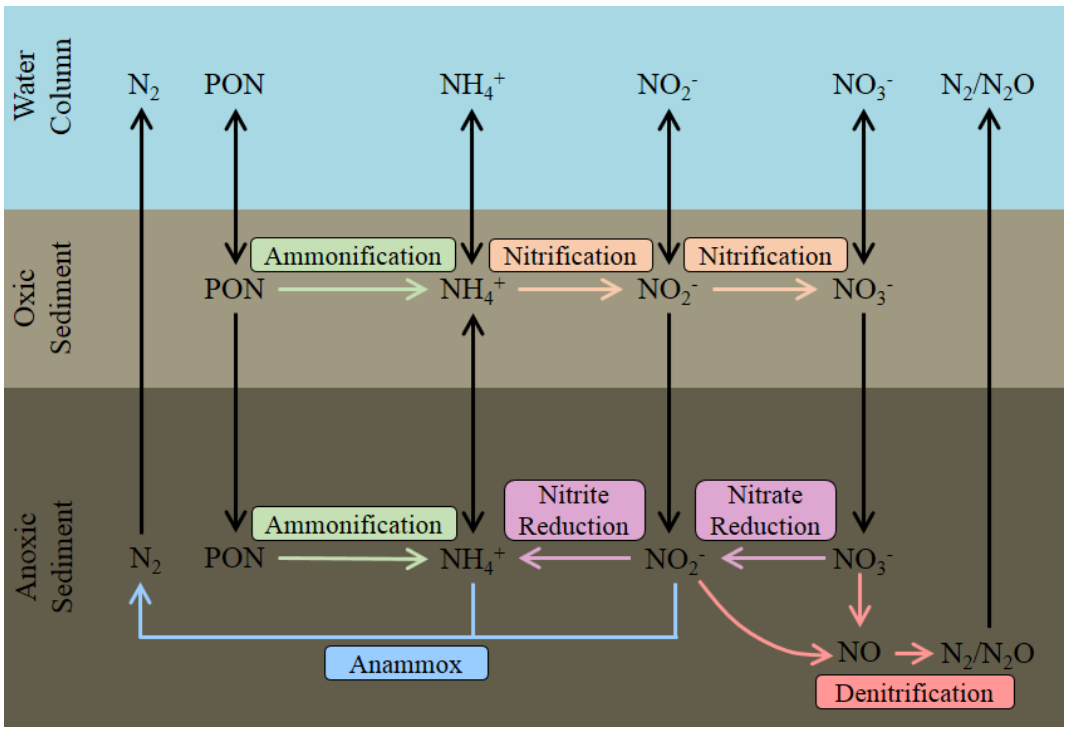

Figure 1.1: The biogeochemical nitrogen cycle in marine sediments, showing processes and chemical transformations forms involved. Figure adapted from Herbert (1999); and Stief (2013).

1.2.3 Phosphorus transformations

Phosphorus (P) in estuarine sediments follows similar patterns to N, in that P is contained in labile particulate organic matter (POM) from the overlying water column (Ruttenberg, 2014) and is either reactive or nonreactive (Paytan & McLaughlin, 2007). Reactive P is generally biologically available in the water column, and found associated with organic matter, iron oxides, and authigenic materials (e.g. carbonate fluorapatite) (Delaney, 1998). Nonreactive P in sediments derives from detrital material from the terrestrial domain (Paytan & McLaughlin, 2007). Burial of P therefore occurs with the burial of organic carbon or as P absorbed with iron oxyhydroxides (Delaney, 1998).

In oxic sediments the majority of organic P is mineralised and precipitates as apatite, to be released as phosphate into pore waters and back into the water column (Anderson *et al.*, 2001). In anoxic sediment P undergoes a series of redox reactions, whereby the reduction of iron oxides results in the release of phosphate into pore waters (Sundby *et al.*, 1992). For the most part, organic matter delivered to the sediment-water interface undergoes regeneration to inorganic forms (Anderson *et al.*, 2001). For example, particulate inorganic P is the result of organic P that has

been remineralised and reprecipitated as calcium fluorapatite (Paytan & McLaughlin, 2007). It is therefore evident that dissolved oxygen differentiates between nutrient cycling processes in the sediment, but dissolved oxygen (or rather the lack of), also has implications on an array of other estuarine functions.

1.3 Ecosystem functioning

Contributing to ecosystem function are the multitude of macrofaunal organisms existing in the upper few centimetres of sediment (Thrush *et al.*, 2006). Benthic fauna have adapted to their environment to create an overarching ecological unit which interacts on both vertical and horizontal spatial scales (Woodward, 1994; Meyer *et al.*, 2015). Fauna create a complex heterogeneous matrix of structure and function, and heterogeneity importantly results in robust ecosystems (Archambault & Bourget, 1996; Herman *et al.*, 1999; Thrush *et al.*, 2012) Macrofauna, through their functional traits, assist in remineralisation and primary production and in turn influence the flux of nutrients to and from the sediment (Thrush *et al.*, 2006; Shull *et al.*, 2009; Crawshaw *et al.*, 2019).

The effects of bioturbation are seen at different scales, such as the disruption of the sediment and organic particle matrix, the transport of sediment, water turbidity, and community composition. Modifications to benthic intertidal areas have the ability to alter pathways and rates of processes such as primary production, nutrient cycling, the redistribution of contaminants and pollutants, and organic matter remineralisation; all of which affect ecosystem functioning (Figure 1.2) (Lohrer *et al.*, 2004; Webb & Eyre, 2004; Thrush *et al.*, 2006).

Bioturbators increase the area available for oxidative exchange, by extending the sediment-water interface (Needham *et al.*, 2010). For example, macrofaunal burrows act to increase the oxic sediment surface areas creating habitat for microorganisms. They can also facilitate the translocation of particles to other reaction zones through the trapping and mixing of sediment (Botto & Iribarne, 2000). Bulldozing species disturb the top the top few centimetres of sediment by continually moving through sediment matrix (Lohrer *et al.*, 2004; Needham *et al.*, 2010). Bulldozing species increase the depth of oxygen penetration in a more uniform way than burrow builders and destabilise sediment through their movement;

therefore increasing the subduction of organic matter, stimulating pore water release and remineralisation (Lohrer *et al.,* 2004; Needham *et al.,* 2010). Some species display functional-plasticity, that is, different sediment environments can change species behaviour and therefore alter their function (Wellnitz & Poff, 2001).

Particular bioturbators can have disproportionate effects on their environment. Jones *et al.* (1994) developed the idea of ecosystem engineering, which refers to organisms that extensively alter the physical structure of their environment, therefore indirectly and/or directly modifying the availability of resources to other species. However this does not necessarily mean that the engineers themselves are a resource to other organisms (Jones *et al.,* 1994). Two categories of ecosystem engineering exist. These are autogenic, (where engineers modify themselves to provide habitat), and allogenic; engineers that transform both non-living and living matter from one state to another (Jones *et al.*, 1994). The extent to which pathways are altered is determined by the species present and their lifestyle mode and traits (Welsh, 2003). Therefore, the different modes of bioturbation have an imperative role in determining the benthic flux of nutrients (Thrush *et al.*, 2006).

A related factor controlling nutrient cycling and benthic flux, is both the quality and quantity of *in-situ* OM (Boynton *et al.*, 2018). A high depositional rate of OM can result in incomplete decay of the labile OM by heterotrophic microorganisms before subsequent burial by benthic organisms (Herbert, 1999). As, such there is establishment of a definitive biogeochemical zonation through sediment depth (Herbert, 1999). It is this zonation that is disrupted by macrofauna, allowing for e^- to be laterally distributed (Kristensen & Blackburn, 1987; Needham *et al.*, 2010).

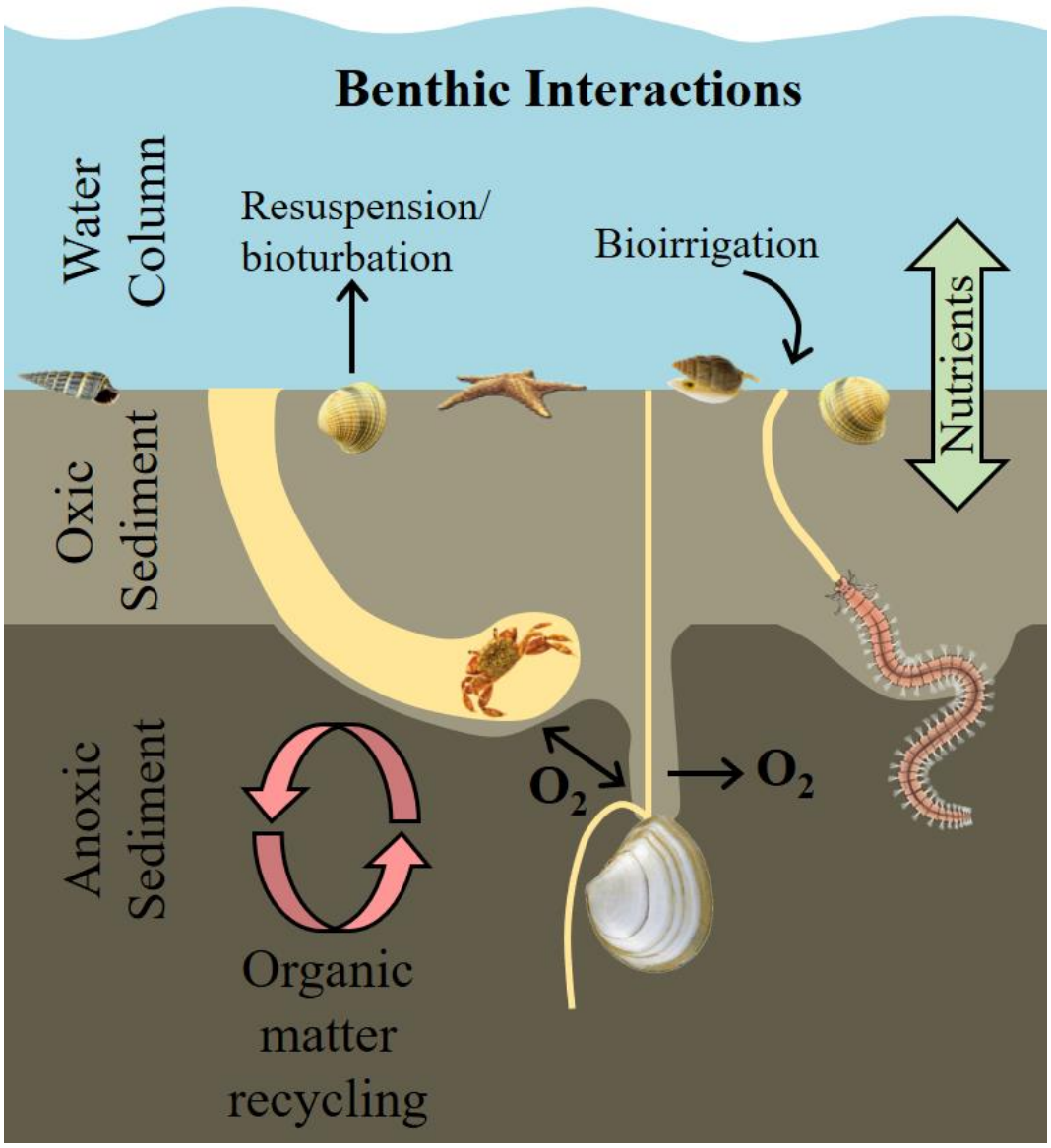

Figure 1.2: Benthic fauna altering multiple processes, including but not limited to, the sediment matrix, oxygen penetration, nutrient fluxes and organic matter cycling.

1.4 Waihī Estuary

Knowing the history of changes within catchments is important for understanding the impacts on the sedimentary and biological environment in estuaries. This study was based in Waihī Estuary, Bay of Plenty, New Zealand.

Waihī Estuary (37º 46' S, 176º 28' E) is a shallow embayment, with an area of approximately 2.4 km^2 (Scholes, 2015; Suren *et al.*, 2016). The system almost completely drains at low tide, leaving only the main channel, which is fed by smaller freshwater catchment drainage channels. Since 1926, channelisation of four main canals that lead into Waihī estuary, namely Whārere, Pukehina,

Kaikokopu and Pangakawa, has occurred to increase flow efficiency (Suren *et al.*, 2016). Before this, the only catchment drainage into the system was via wetlands to the south of the estuary (Park, 2016). The stream redirection and subsequent loss of wetlands resulted in contaminants (e.g. nutrients and sediments) bypassing an important filtration process. Waihī Estuary is one of the smallest estuaries in the Bay of Plenty region but is the end point for waterways in the 365 km^2 Pongakawa catchment (Suren *et al.*, 2016). The intensification of dairy farming in the Pongakawa catchment has resulted in elevated levels of faecal concentration in the estuary (Scholes, 2015). The Bay of Plenty Regional Council reported the transport of high levels of nutrients and bacteria into the estuary (Suren *et al.*, 2016). However, the better flushed parts of Waihī Estuary still appear to be relatively healthy, supporting shellfish beds that are regularly harvested by locals.

1.5 Study objectives

To date, there have been very few field studies that have examined the impacts of eutrophication across a gradient of change, which is important if we are to better understand 'real world' system dynamics. The key objective of this study was to examine how the intertidal area of Waihī Estuary changes as we move from healthier to more impacted sites. To do this, I used space as a proxy for time and sampled across the spatial extent of Waihī Estuary. Changes in functioning associated with both sedimentary and macrofaunal drivers will give some insight in to how environmental degradation proceeds as eutrophication pressures increase. I wish to identify what functional shifts occur as degradation increases and what explanatory variables exert the most control over solute exchanges.

My key goals are therefore:

- To determine how the sediment environment varies across the gradient and if this alters the macrofaunal community structure.
- To investigate the small-scale differences in ecosystem function along the gradient and what drives site level change.
- To elucidate how eutrophication alters ecosystem function at a system wide scale and what interactions and drivers are responsible for the resultant outcomes.

Chapter Two

Methods

2.1 Experimental design

Solute flux measurements are estimates of the exchange rates of dissolved materials (e.g. nitrogen, ammonium, phosphorus and oxygen) between differing areas (Tengberg *et al.*, 2004); in this case, between sediment and the overlying water column. Fluxes of key solutes, such as oxygen, indicate the net outcomes of important ecosystem processes such as primary production (the conversion of sunlight energy into biomass), community respiration and organic matter remineralisation. Seven sites within Waihī Estuary (37º 46' S, 176º 28' E; Figure 2.1) were chosen to encompass changes in organic matter loading and associated stressors based on observable cues, including sediment mud content, dominant bioturbator(s), apparent redox potential discontinuity depth (aRPD), and proportion of filamentous red algae cover (*Gracilaria* spp.). Sites ranged in location from near the mouth of Waihī Estuary through to the upper reaches and covered a range of faunal assemblages.

Sampling occurred in two expeditions during February (late summer) 2018 to coincide with midday high tides, in order to capture the greatest light intensity (and hence benthic productivity). Sites 2, 4 and 5 were sampled on 7th to 8th, and sites 1, 2, 6 and 7 were sampled on 19th to 21st. Weather for sites 1 to 5 and 7 was overcast, with periods of clear skies; site 6 was windy with spells of rain.

Figure 2.1: Satellite image of Waihī Estuary showing site locations (sites 1 to 7), channelized canals, and immediate surrounding land use. Satellite image: Google Earth.

2.1.1 **Chamber incubations**

A common method of quantifying solute fluxes is with chambers (Needham *et al.*, 2011; Thrush *et al.*, 2017; Douglas *et al.*, 2018; Drylie *et al.*, 2018), where sediments are incubated together with overlying water and changes in water chemistry (solute concentrations) over time are tracked. Here, following Lohrer *et al.* (2016), benthic incubation chambers were used to enclose an area of 0.25 m^2 with ~37 L of overlying water. The chambers consisted of 50 cm x 50 cm square aluminium bases with a depth of 15 cm. The bases were pressed 5 to 10 cm into the sediment (depending on the site) and topped with removable transparent Perspex lids. Chamber lids were attached to the bases after approximately 30 cm of flood tide inundation and internal air bubble removal via air suction tubes. Exhaust and intake ports were incorporated into the lids to allow for syringe samples to be taken, and pressure compensation through water replenishment. Inside each chamber, a SeaBird battery powered electronic stirrer motor, a

dissolved oxygen logger (PME miniDOT oxygen sensor, reading once per minute; Precision Measurement Engineering, 2014) and a HOBO light sensor (ONSET, 2018), were attached to the chamber walls (Figure 2.2). Stirrer motors placed inside, were pumping intermittingly for five seconds every 45 seconds to disrupt stratification within the chambers, which can affect flux measurements.

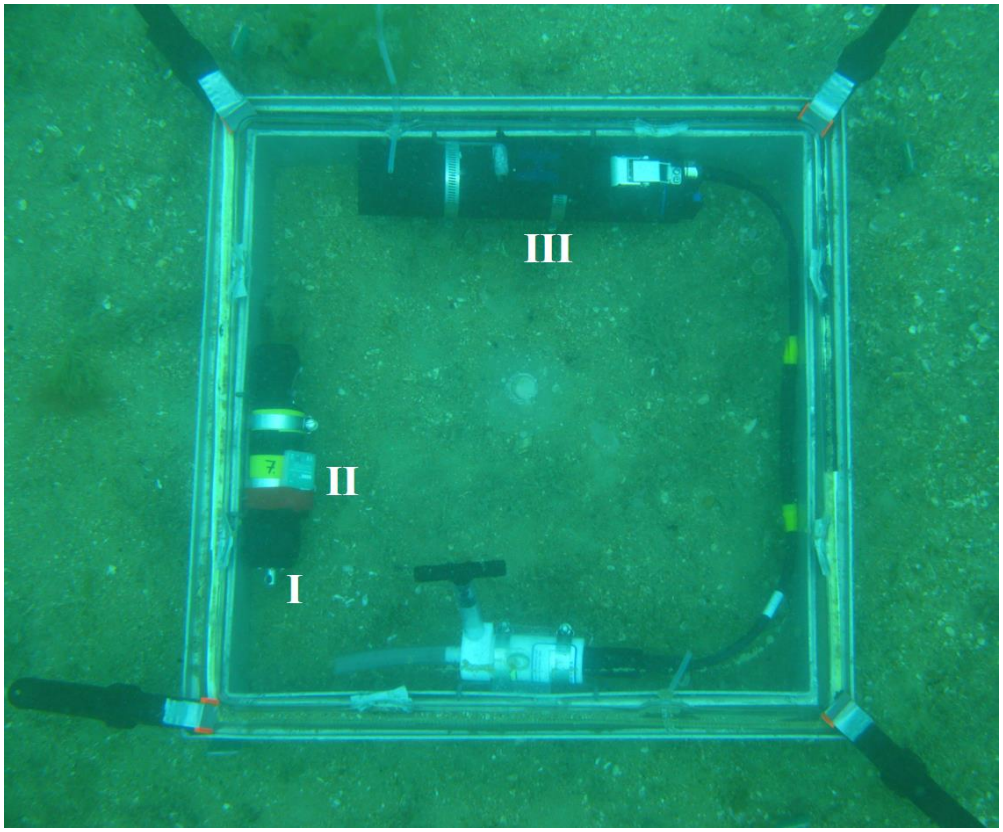

Figure 2.2: Internal chamber layout showing; I) dissolved oxygen logger with II) Hobo light logger attached, III) water pump and battery pack. Photo: NIWA archive.

At each site, 10 benthic chambers were positioned parallel to the incoming tide to ensure each chamber was covered for a similar duration at the same water depth. Chambers were set out in light and dark pairs (n=5), where dark chambers were covered by a shade-cloth, preventing light penetration (Figure 2.3). Chambers were incubated from the time lids were attached, until the ebb tide lowered to beneath the chamber lids. By using this method, we were able to quantify oxygen production via photosynthesis in light chambers, while eliminating the effects of photosynthetic processes in dark chambers. This allowed for estimates of total community respiration (i.e. microbial activity and benthic fauna) through the measurement of oxygen removal. Dark chambers also aid to control differences in light intensity from variation in water turbidity, water depth, and weather across the

days sampled. Three HOBO light loggers were distributed throughout each site to record light intensity (at 5-minute intervals) for the duration of the chamber incubations. To compensate for water column productivity, three sets of paired light and dark bottles filled with ambient seawater (volume = 1.5 L) were distributed throughout each site and incubated at the same time as the chambers.

The four main solutes analysed were dissolved oxygen (DO), ammoniacal nitrogen (NH_4^+-N), dissolved reactive phosphorus (PO_4^{3-}-P), and nitrate and nitrite (in combination, NO_x-N). Seawater present inside the chambers was collected through ports attached to sampling tubes with luer-lock valves. From each chamber, 60 ml water samples were collected by syringe (first discarding the volume of water in the tubing, ~ 120 ml), at the beginning and end of the incubation period. Additional to *in-situ* DO loggers, a point DO reading was measured from each chamber water sample using a PreSens FIBOX 3 LCD Trace v7 optical dissolved oxygen probe (PreSens, 2009). Water samples were then filtered through a 1.1 µm Whatman GF/C filter (to remove phytoplankton and microbes that could further alter nutrient concentrations), put on ice, and stored at -20˚C, until analysis.

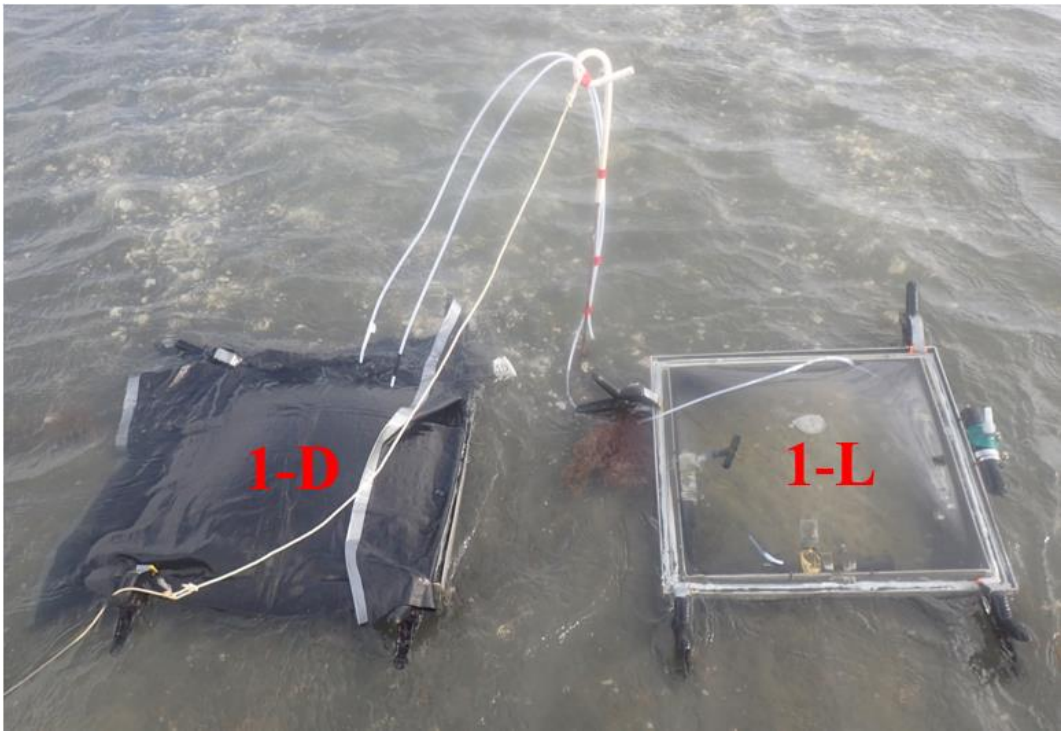

Figure 2.3: Light and dark paired chambers, with lids, shade cloth and tubing attached. Photo: NIWA archive.

2.1.2 **Sampling of co-variables**

Prior to incubation, three pooled sediment cores (2.6 cm diameter corer, pushed 2 cm deep) were collected for porosity analysis adjacent to, but outside the enclosed area of each paired set of chambers at low tide. Macrofauna and other sediment samples were collected post-incubation from the inside of each chamber using a 13 cm diameter core pushed 15 cm deep into the sediment, enabling quantification of the benthic community structure within each chamber. Macrofauna cores were sieved on site (mesh size = 500 µm) and preserved in 70% isopropyl alcohol, with the later addition of 1% rose bengal to stain biological tissue. For assessment of organic matter content (OM), chlorophyll *a* (chl *a)* analysis and grain size, six sediment cores (2.6 cm diameter corer, pushed 2 cm deep) were collected from each chamber and split into two pools of sediment. Sediment samples were stored in the absence of light at -18˚C to prevent degradation of chl *a* and OM. The aRPD depth was measured by taking a cross sectional photo of a sediment core inside a syringe corer (Figure 2.4). Three aRPD photos were taken per site, and three measurements within each photo were averaged to gauge the aRPD depth. Photos were scaled and measured using SketchUp (Trimble Inc, 2019). To measure the percentage *Gracilaria* spp. (macroalgae) cover across the sites, photos were taken of every chamber base bedded into the sediment. Within each photo, chamber bases were divided into nine equal segments, and the proportion of macroalgal cover was estimated for each segment then added together and averaged across each site.

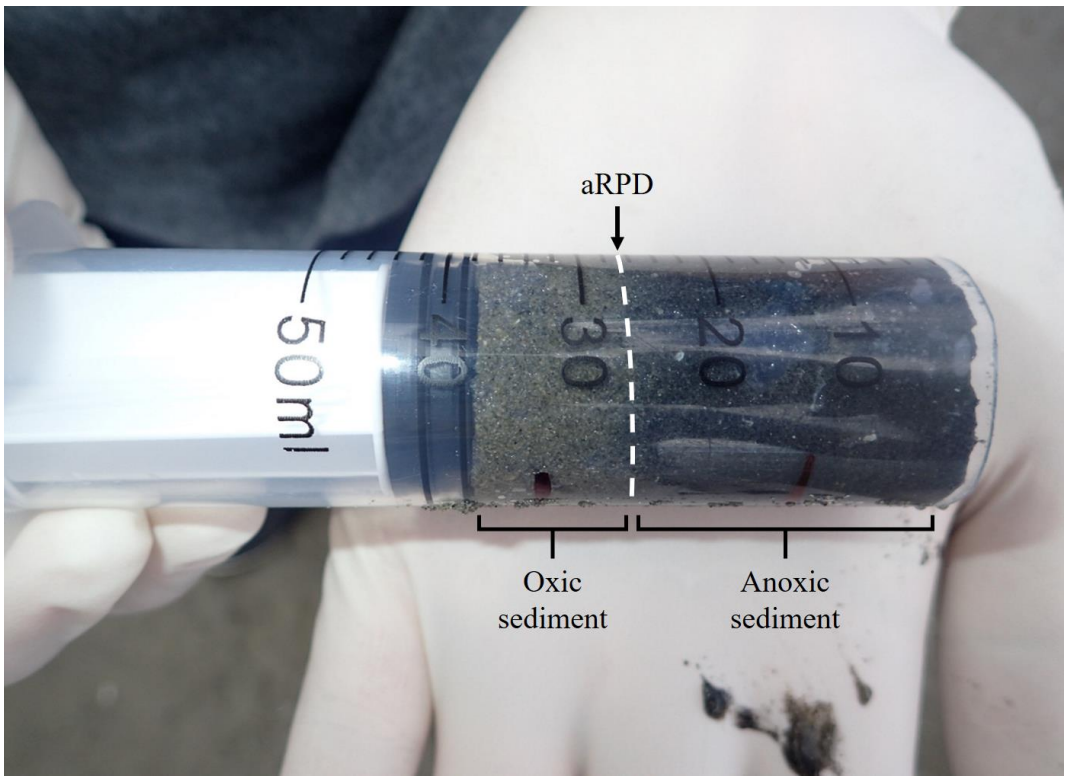

Figure 2.4: Syringe core showing a site 1 depth profile of oxic sediment, anoxic sediment, and the apparent redox potential discontinuity (aRPD) zone between the two sediment layers.

2.1.3 Laboratory analyses

Macrofauna were separated into different size classes by sieving (0.5 to 1 mm, 1 to 2 mm and >2 mm), and all stained biological tissue observed was removed. Macrofauna were then identified to the lowest taxonomic level practicable (generally to species level) using a dissecting microscope (Leica M80 Stereo Microscope with Ergo Wedge and LED light attachments; Leica Microsystems, 2016). Samples were identified according to NIWA (National Institute of Water and Atmosphere) standards and quality control checked by NIWA staff.

For measurement of chl *a* and phaeophytin concentration (phaeo; a degradation product of chl *a*), a University of Waikato standard operational procedure for marine sediment was used (modified from Arar & Collins, 1997). In short, subsamples of homogenised sediment were freeze dried, weighed to 15 grams, added to 10 ml of 90% buffered acetone, and steeped at 4˚C overnight. Samples were then centrifuged at 3300 rpm for 10 minutes. Extracted chl *a* was measured before and after hydrochloric acidification (0.15 N HCl) using a Turner 10-AU

fluorometer. These two values (before and after acidification) were used to calculate the concentrations of chl *a* and phaeophytin.

Sediment samples (~15 ml) were digested in 10% hydrogen peroxide to remove organic matter. After two weeks of digestion, 10 ml of Calgon water softener was added, before being sonicated for 30 minutes to aid with sediment dispersal and disaggregation (Singer *et al.*, 1988). Samples were measured using a Malvern Mastersizer 3000 Lazersizer set to 3000 rpm, with a refractive index of 1.5 and an absorption of 0.2 (Singer *et al.*, 1988). This method allows for the quantification of grain size distribution and proportion (i.e. mud to sand content), as well as the overall median grain size.

Sediment organic matter content was measured by percentage weight loss on ignition. Samples were dried at 60˚C until constant mass was achieved and then combusted at 550˚C for four hours to remove the ash fraction (Heiri *et al.*, 2001). Porosity was analysed by comparing sediment wet weight to sediment dry weight, after sediment had reached constant mass at 60˚C. Analysis of dissolved inorganic nutrients was carried out in the NIWA Hamilton chemistry laboratory, using standard operational methods for seawater on an Astoria-Pacific 300 series segmented flow auto-analyser.

2.2 Flux calculations

The change in water chemistry between initial and final samples was used to calculate solute fluxes. All fluxes within each chamber were calculated using the following equation, and measured in units of μmol m^{-2} hr^{-1}:

$$Flux = \frac{(\Delta f \times V)}{(A \times \Delta T)},$$

where Δf is the concentration change of the measured solute (μmol L^{-1}), V is the volume of seawater in each chamber (L), A is the area of seafloor covered by each chamber base (0.25 m^2), and ΔT is incubation time between initial and final samplings (decimal hours). Through improper lid attachment and/or gear failure, two chambers (Site 1 and 4 D dark) were identified to have leaks. Measurements from these chambers were therefore excluded from flux analyses. DO measurements were used to calculate gross primary production (GPP) which is the

total chemical energy created by primary producers (i.e. photosynthetic organisms such as microphytobenthos and sea grass) per unit area, per unit time (Sigman & Hain, 2012). GPP was calculated as the difference between dark and light DO fluxes, i.e. subtracting the dark chamber DO flux from the light chamber DO flux. Given the difference in macroalgal and microphytobenthos cover, GPP was then normalised by the biomass of sediment chl *a*, to provide a measure of photosynthetic efficiency ($GPP_{chl\ a}$).

2.3 Statistical Analyses

Scatterplots and site averaged bar charts were used to visualise preliminary relationships of solute fluxes, GPP and sediment-macrofauna trends across the sampled gradient. Permutational analyses of variance (PERMANOVA; Anderson *et al.*, 2008) were conducted on Euclidian distance resemblance matrices of the solute fluxes to examine differences across all sites. Pair-wise post-hoc tests were then used to break down significant differences in solute fluxes between sites.

Univariate macrofaunal statistics were produced to compare changes in site community composition, and included macrofauna abundance (N), taxonomic richness (S) and Shannon-Weiner diversity index (SW). N and S were calculated by totalling the number of individual organisms and the number of species (respectively) per macrofauna core and creating site averages. SW was calculated for each macrofauna core using the following equation:

$$H' = -\sum_{i=1}^{S} \pi\ ln\pi,$$

where the proportion of species (*i*) was calculated relative to the total number of species (*pi*) and multiplied by the natural log (*ln*) of π. This product was then summed across all the species and multiplied by -1 (Shannon, 1948). For further analyses, macrofauna abundance data were square-root transformed to correct for skewness of abundant and rare species (Anderson *et al.*, 2008). Counts of all species were combined into a Bray-Curtis resemblance matrix with site as a factor, before generating a non-metric multidimensional scaling plot (nMDS) to visualise community structure. Principal component ordination (PCO) plots with vector overlays of sediment properties were used to visualise explanatory variables influencing the macrofauna community structure and to better inform further

analyses. SIMPER analysis was also conducted to ascertain the species most influential to (dis)similarities within and between sites (cumulative contribution >50%).

Multivariate Distance based Linear Models (DistLM) were used to understand drivers of solute fluxes across the environmental gradient. Response and explanatory variables were all normalised prior to analysis. Response variables used in the analysis were sediment oxygen consumption (SOC; dark chamber DO flux), $GPP_{chl\ a}$, and dark chamber solute fluxes of NH_4^+-N, PO_4^{3-}-P and NO_x-N. Explanatory variables were sediment parameters, univariate macrofaunal statistics, and untransformed significant species from SIMPER analyses. Collinearity amongst explanatory variables was avoided for model robustness, minimising over inflation of explanatory variable standard error. Collinearity of explanatory variables was checked using Pearson's correlation matrix, and where correlations were >0.85, the variable explaining the least variation was excluded; OM was always fitted first. By using only dark chamber fluxes in the DistLM analyses, photosynthetic uptake (via microphytobenthos and phytoplankton) of dissolved nutrients was removed, enabling better discernment of the effects of macrofauna on solute fluxes.

To achieve the most parsimonious model that also explained the highest explanatory variable proportions, stepwise elimination routines were used with 999 permutations, employing the Akaike information criterion corrected (AIC_C). AIC_C was the preferred selection criterion due to its ability to handle a small samples number (N) relative to the amount (p) of explanatory variables ($N/p < 40$) (Anderson *et al.*, 2008). DistLM results were then visualised with distance-based redundancy analysis (dbRDA) (Anderson *et al.*, 2008).

Exploratory histograms, scatterplots, bar charts and univariate statistics were carried out using STATISTICA version 13 (TIBCO Software Inc, 2018) and Microsoft Excel (2016). All nMDS, PERMANOVA, PCO, SIMPER, DistLM and associated functions were conducted using PRIMER 7 (Version 7.0.13) with PERMANOVA + 1 add-on (Clarke & Gorley, 2015).

Chapter Three

Results

3.1 Sediment variables

From site 1 to 7, sedimentary variables sampled in Waihī Estuary demonstrated a distinct gradient (Table 3.1). Organic matter content (OM) is an important measure of eutrophication, and elevated mud content (mud %) is a known consequence of eutrophication (Nixon, 1995; Rabalais *et al.*, 2009). These variables (OM and mud %) were highly correlated (R = 0.94; Table 3.2) with an increase in OM linked to an increase in mud %. Across sites, OM ranged from 2.3 to 8.3%, and mud % ranged from 3.6 to 90.5%. Also correlated to mud % was median grain size (Med GS; R = 0.89), which decreased by 190 µm from the least muddy site (site 1 = medium sand) to the muddiest site (site 7 = medium silt) (Wentworth, 1922). However, the decrease in Med GS was not linear, for example, site 5, which had a similar mud content to site 4, had the largest Med GS of 247 µm (medium sand), while sites 1 to 4 range from 155 to 208 µm Med GS (fine sand). Porosity (Por), which was negatively correlated to OM (R = -0.77), remained similar across sites 1 to 5 and increased at sites 6 and 7, giving a total range of 0.29 Por.

Chlorophyll *a* (chl *a*) was similar at four of the seven sites (sites 1, 2, 3 and 6). It was lowest at sites 4 and 5 (10.5 to 13 µg g^{-1} sediment respectively), and highest at site 7 (61.5 µg g^{-1} sediment). Phaeophytin (phaeo; a degradation product of chl *a*) was highly correlated to chl *a* (R = 0.86) and OM (R = 0.83). Like chl *a*, phaeo was also lowest at sites 4 and 5 (8.3 and 8.0 µg g^{-1} sediment respectively) and highest at site 7 (128.6 µg g^{-1} sediment). The peak in chl *a* and phaeo at site 7 also corresponded with the highest percent *Gracilaria* spp. cover (69%), and the lowest apparent redox potential discontinuity (aRPD) depth of <3 mm. Sites 1, 2 and 3 had little *Gracilaria* spp. cover (<3%), but higher amounts chl *a* content (19.9 to 25.2 µg g^{-1} sediment). *Gracilaria* spp. cover was positively correlated to OM (R = 0.74), while aRPD depth was negatively correlated to OM (R = -0.72) indicating an increase in OM was associated with an increase in *Gracilaria* spp. and a shallower aRPD depth. aRPD was deepest at site 4 (23 mm) and shallowest at site 7 (2 mm) (Table 3.1).

Table 3.1: Site averaged environmental variables (± 1 SD; units specified). Med GS: median grain size, mud %: mud content, OM: organic matter content, chl *a*: chlorophyll *a*, phaeo: phaeophytin, aRPD: apparent redox discontinuity potential.

Sediment properties	**Site 1**	**Site 2**	**Site 3**	**Site 4**	**Site 5**	**Site 6**	**Site 7**
Med GS (µm)	208 (± 9)	170 (± 10)	201 (± 12)	155 (± 11)	247 (± 26)	57 (± 11)	18 (± 5)
Mud % (< 63 µm)	3.6 (± 0.9)	7.5 (± 1.3)	8.7 (± 2.0)	18.0 (± 3.4)	19.5 (± 4.6)	55.0 (± 7.1)	90.5 (± 7.2)
OM (%)	2.3 (± 0.1)	2.9 (± 0.1)	2.6 (± 0.1)	2.8 (± 0.1)	2.7 (± 0.2)	5.1 (± 0.1)	8.3 (± 0.1)
Porosity	0.56 (± 0.08)	0.56 (± 0.03)	0.54 (± 0.02)	0.54 (± 0.01)	0.54 (± 0.02)	0.66 (± 0.02)	0.83 (± 0.07)
Chl *a* (µg g^{-1} sediment)	23.9 (± 3.1)	19.9 (± 5.2)	25.2 (± 4.7)	10.5 (± 1.4)	13.0 (± 2.0)	21.3 (± 3.1)	61.5 (± 40.8)
Phaeo (µg g^{-1} sediment)	10.4 (± 4.1)	11.3 (± 5.1)	9.3 (± 2.2)	8.3 (± 2.0)	8.0 (± 2.0)	14.1 (± 2.3)	128.6 (± 79.1)
aRPD depth (mm)	12 (± 4)	12 (± 1)	13 (± 3)	23 (± 8)	13 (± 3)	9 (± 1)	2 (± 1)
Gracilaria spp. cover (%)	0	1 (± <0.00)	1 (± 2)	0.2 (± 0.5)	7 (± 9)	3 (± 2)	69 (± 27)

Table 3.2: Pearson's correlation coefficients of environmental and biological variables. Correlations above 0.85 are shown in bold*.

	Med GS (µm)	Mud %	OM (%)	Porosity	Chl *a* (µg/g)	Phaeo (µg/g)	aRPD (mm)	*Gracilaria* spp. (%)	SW (H')	N (core^{-1})	S (core^{-1})	A. stu<10 mm	A. stu>10 mm	*M. lil* <10 mm	*M. lil* >10 mm	Total *A. stu*	Total *M. lil*	*P* spp.	*C* spp.
Med GS (µm)																			
Mud %	**-0.89**																		
OM (%)	**-0.85**	**0.94**																	
Porosity	-0.77	0.84	0.77																
Chl *a* (µg/g)	-0.50	0.59	0.70	0.35															
Phaeo (µg/g)	-0.60	0.73	0.83	0.53	**0.86**														
aRPD (mm)	0.57	-0.70	-0.72	-0.47	-0.60	-0.60													
Gracilaria spp. (%)	-0.60	0.76	0.74	0.57	0.48	0.68	-0.66												
SW (H')	0.34	-0.51	-0.40	-0.43	-0.23	-0.32	-0.06	-0.32											
N (core^{-1})	0.43	-0.61	-0.60	-0.64	-0.37	-0.47	0.73	-0.55	0.04										
S (core^{-1})	0.53	-0.77	-0.69	-0.69	-0.41	-0.57	0.35	-0.64	0.79	0.53									
A. stu <10 mm	0.38	-0.44	-0.37	-0.64	-0.03	-0.19	0.06	-0.24	0.45	0.41	0.55								
A. stu >10 mm	0.29	-0.37	-0.33	-0.41	-0.19	-0.25	0.46	-0.26	0.12	0.40	0.23	0.10							
M. lil <10 mm	0.34	-0.47	-0.44	-0.55	-0.25	-0.28	0.66	-0.33	-0.05	0.75	0.29	0.42	0.42						
M. lil >10 mm	0.43	-0.59	-0.46	-0.67	-0.08	-0.26	0.04	-0.33	0.74	0.33	0.74	0.68	0.09	0.25					
Total *A. stu*	0.39	-0.46	-0.39	-0.66	-0.04	-0.20	0.08	-0.26	0.45	0.43	0.56	**0.99**	0.16	0.44	0.68				
Total *M. lil*	0.46	-0.64	-0.55	-0.74	-0.23	-0.34	0.53	-0.41	0.31	0.73	0.57	0.64	0.37	**0.89**	0.66	0.66			
P spp.	0.01	-0.07	-0.17	0.10	-0.33	-0.20	0.69	-0.23	-0.57	0.54	-0.15	-0.27	0.13	0.41	-0.44	-0.26	0.11		
C spp.	0.17	-0.32	-0.28	-0.40	-0.10	-0.26	-0.04	-0.33	0.51	0.30	0.56	0.77	-0.09	0.17	0.51	0.76	0.37	-0.24	

**For later reference, correlations above 0.85 are marked for the purposes multicollinearity in DistLM models.*

3.2 **Biological variables**

A non-metric multi-dimensional scaling (nMDS) plot was constructed to visualise variation in macrofauna community structure within and among sites (Figure 3.1). Site 1 exhibited the most homogeneous community structure (samples from site 1 clustered tightly together in Figure 3.1), and site 7 the most heterogeneous community structure (site 7 samples were relatively widely dispersed in the nMDS plot). However, within site variance did not uniformly increase from site 1 to 7. For example, site 2 showed greater heterogeneity than sites 3 and 4.

Samples from each site clustered distinctly together in ordination space and did not overlap with samples from other sites, with the possible exception of samples from sites 5 and 6. PERMANOVA (Table 3.3) and post-hoc tests confirmed that all sites were significantly different from one another ($p = 0.001$). Sites 1 to 3 were relatively close together in ordination space, as were sites 4 to 6, all of which were separated from site 7.

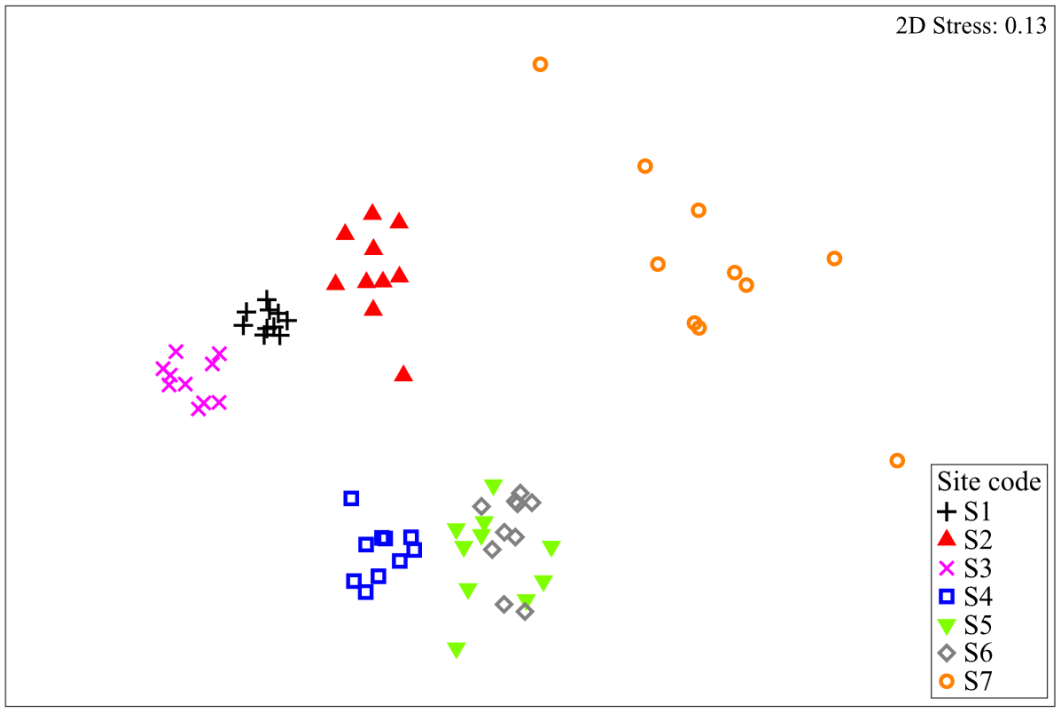

Figure 3.1: Non-metric multi-dimensional scaling (nMDS; Bray-Curtis resemblance) of square-root transformed macrofauna community structure. Each point represents one macrofauna core, the different colours and shapes represents differing sites (S1 – S7).

Table 3.3: PERMANOVA test (Bray-Curtis resemblance matrix, 999 permutations) on macrofauna community structure as a function of sites. Pair-wise post-hoc tests show significant differences ($p < 0.05$) across all sites.

Source	dF	MS	Pseudo-F	p(perm)	Pair-wise tests
Site	6	21326	35.01	0.001	1≠2≠3≠4≠5≠6≠7
Residual	63	609			

The highest average taxonomic richness (S) was seen at sites 1 and 2 (17 taxa core^{-1}) and the lowest at site 7 (4 taxa core^{-1}; Table 3.4). Taxa richness and Shannon-Weiner diversity (SW) were relatively strongly correlated (R = 0.79; Table 3.2), and both generally decreased with increasing eutrophication. Macrofauna abundance (N), was on average highest at site 4 (300 inds. core^{-1}) and lowest at site 7 (17 inds. core^{-1}). Although there was a relatively linear decrease in S across sites, this was not the case with N. As S decreased and key species were lost, other species became dominant. SIMPER analysis (Table 3.5) of species dissimilarity between sites showed an increase in macrofauna community dissimilarity from site 1 to sites 3, 5 and 7 as the eutrophic gradient increased. The species contributing to dissimilarities in community composition among sites are listed in Table 3.5. Although most species became less abundant as eutrophication increased (notably *A. stutchburyi*), a few (e.g. *Prionospio aucklandica*, *Anthropleura aureoradiata*, and *Paracorophium* spp.) increased in number. Total abundance was only significantly different at sites 1 and 7, which were of greatest dissimilarity (89%). Site 7 had the lowest S, and site 4 had the lowest SW diversity score.

The low SW diversity score seen at site 4 was likely driven by low evenness, with *Paracorophium* spp. reaching upwards of 300 individuals per macrofauna core. Figure 3.3 also highlights that *Paracorophium* spp. were rare at sites 1 and 2, and completely absent at site 3. One of the key species lost with increasing eutrophication was *Macomona liliana*, with adult *M. liliana* (>10 mm shell length) absent from sites 4 to 7. SIMPER analysis (Table 3.6) suggested that another key species, *A. stutchburyi*, decreased from site 1 to 4. The loss of *M. liliana* >10 mm, and the reduction of *A. stutchburyi* at site 4 coincided with a shift in two of the parallel issues associated with eutrophication; an increase in sediment OM and mud %. As evidence of eutrophication increased, a reduction in macrofaunal abundance was observed, particularly between sites 4 and 5, where a sharp decline was seen.

Table 3.4: Site averaged macrofauna variables (± 1 SD; units specified). N: macrofauna abundance, S: taxonomic richness, SW: Shannon-Weiner diversity index.

	Site 1	Site 2	Site 3	Site 4	Site 5	Site 6	Site 7
N (core^{-1})	241 (± 33)	132 (± 42)	244 (± 70)	300 (± 102)	98 (± 39)	120 (± 41)	17 (± 23)
S (core^{-1})	17 (± 2)	17 (± 2)	15 (± 2)	11 (± 2)	9 (± 2)	11 (± 2)	4 (± 2)
SW (H')	2.1 (± 0.1)	2.3 (± 0.2)	1.7 (± 0.1)	0.9 (± 0.4)	1.2 (± 0.5)	1.5 (± 0.2)	1.0 (± 0.4)

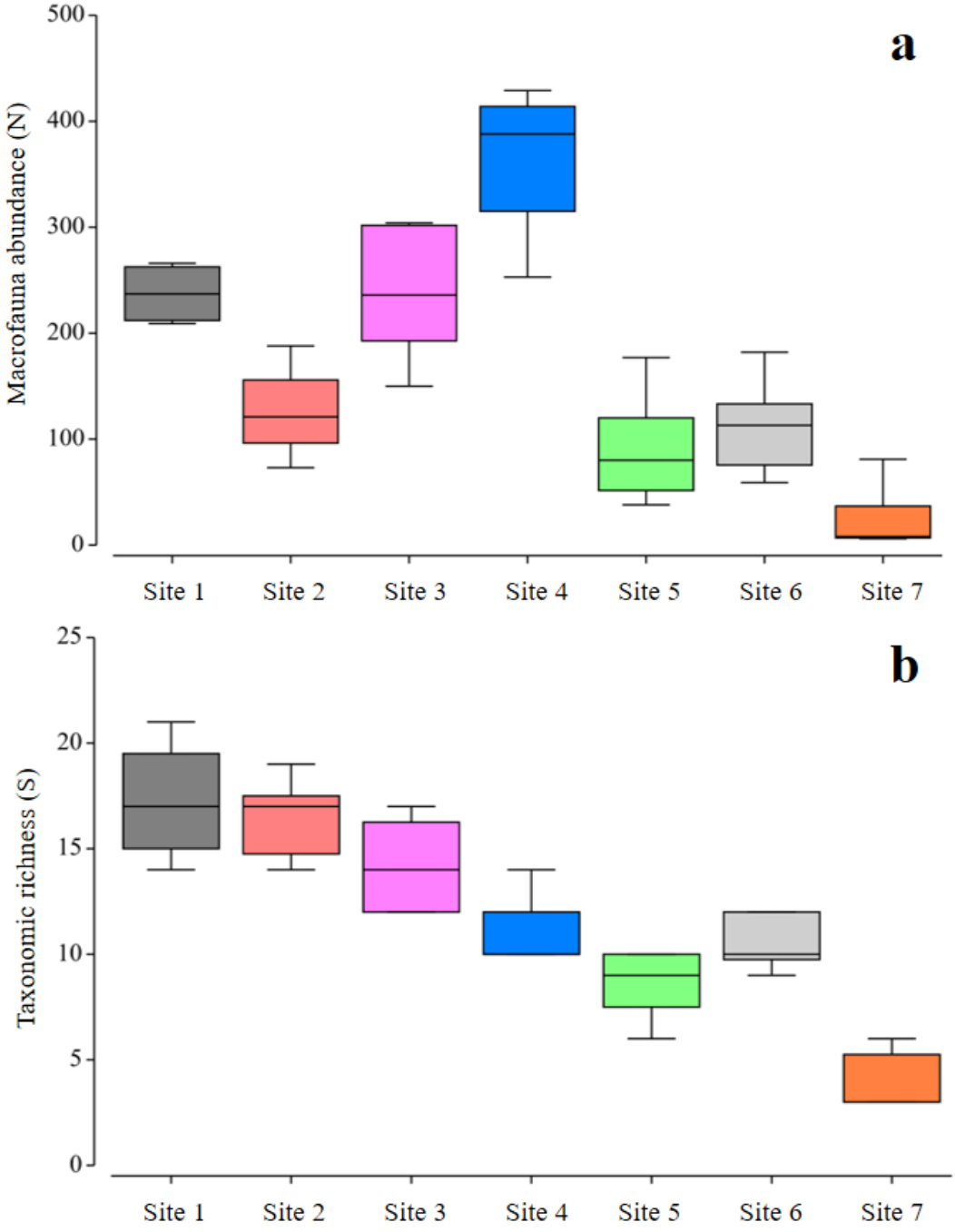

Figure 3.2: (a) Macrofauna abundance (N); and (b) taxa richness (S); averaged at each site in both light and dark chambers. Boxes show median, 25% and 75% distributions, with whiskers representing maximum and minimum values.

Table 3.5: SIMPER analysis (Bray-Curtis similarity) of square-root transformed macrofauna data comparing site 1 to sites 3, 5 and 7 to show that as the sampled gradient increases in apparent eutrophication pressure, there was an increase in the dissimilarity of the macrofaunal community structure.

	Species	Site dissimilarity (%)	Average abundance		Species dissimilarity (%)	Contribution (%)	Diss/SD
Sites 1 & 3		**43.24**	**Site 1**	**Site 3**			
	Prionospio aucklandica		5.03	11.27	6.45	14.91	3.58
	Austrovenus stutchburyi		9.32	5.03	4.48	10.35	3.80
	Ceratonereis spp.		5.90	2.69	3.33	7.70	3.00
	Oligochaeta		4.11	1.41	3.23	7.48	1.72
	Microspio maori		2.85	0.20	2.74	6.35	4.08
	Anthropleura aureoradiata		2.25	4.48	2.53	5.85	1.49
Sites 1 & 5		**76.68**	**Site 1**	**Site 5**			
	Austrovenus stutchburyi		9.32	0.91	11.46	14.95	7.01
	Paracorophium spp.		0.10	7.63	10.22	13.33	3.13
	Ceratonereis spp.		5.90	1.39	6.13	7.99	4.38
	Prionospio aucklandica		5.03	0.57	6.10	7.96	3.96
	Macomona liliana		3.95	0.40	4.82	6.28	4.60
Sites 1 & 7		**88.7**	**Site 1**	**Site 7**			
	Austrovenus stutchburyi		9.32	0.20	15.84	17.86	7.90
	Ceratonereis spp.		5.90	0.89	8.71	9.82	4.96
	Prionospio aucklandica		5.03	0.00	8.71	9.81	7.67
	Macomona liliana		3.95	0.10	6.66	7.51	5.91
	Austrominius modestus		2.91	0.00	4.97	5.60	1.73

Table 3.6: SIMPER analysis (Bray-Curtis similarity) of square-root transformed macrofauna data comparing site 1 to site 4.

	Species	Site dissimilarity (%)	Average abundance		Species dissimilarity (%)	Contribution (%)	Diss/SD
		69.80	**Site 1**	**Site 4**			
Sites 1 & 4	*Paracorophium* spp.		0.10	15.24	17.19	24.62	4.76
	Austrovenus stutchburyi		9.32	2.48	7.82	11.2	6.09
	Ceratonereis spp.		5.90	1.53	5.02	7.19	3.89
	Austrominius modestus		2.91	0.00	3.29	4.71	1.71
	Oligochaeta		4.11	1.55	3.19	4.57	1.70

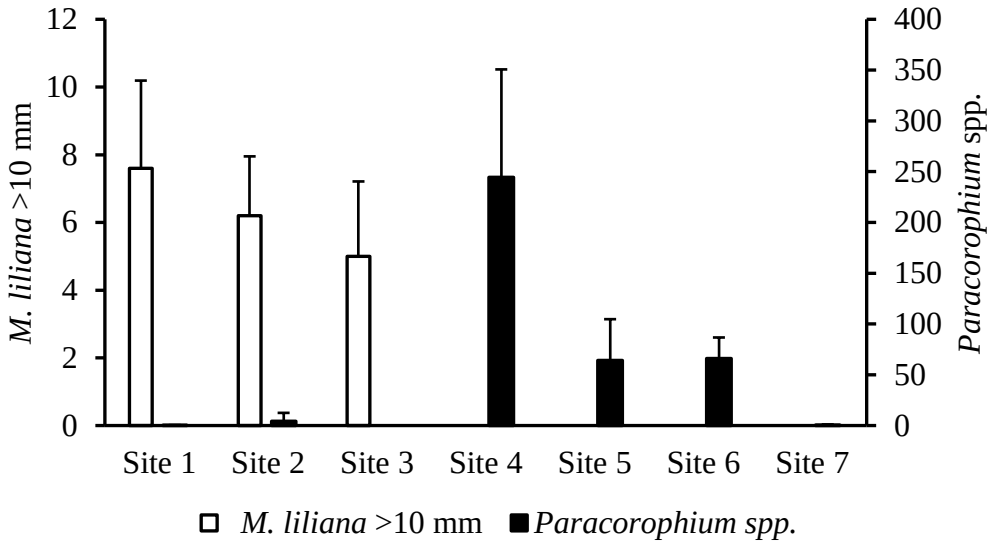

Figure 3.3: *Macomona liliana* >10 mm (left axis) and *Paracorophium* spp. (right axis) abundance across all sites (+SD).

3.3 **Sediment – organism interactions**

To examine the interactions between sediment properties, macrofaunal distribution and community composition, a Principal Coordinate Analysis (PCO) of macrofauna data was performed. The first axis (PC1) explained 33.7% of the variability in the data, and the second axis (PC2) explained 21.8% (Figure 3.4). As with the previous MDS analysis (Figure 3.1), PCO revealed three groups, where sites 1 to 3 were separated from sites 4 to 6, which were all separated from site 7. However, within site heterogeneity of site 7 was reduced. Macrofauna at site 7 were associated with elevated mud %, OM and P (as shown by the vectors on Figure 3.4). Med GS was negatively correlated to mud %, OM and P, indicating that macrofaunal communities at sites 1 to 3 may be influenced by increases in Med GS, and reduction of mud %, OM and P. A decrease in chl *a* helped distinguish macrofaunal communities at sites 4 to 6 from the rest of the sites.

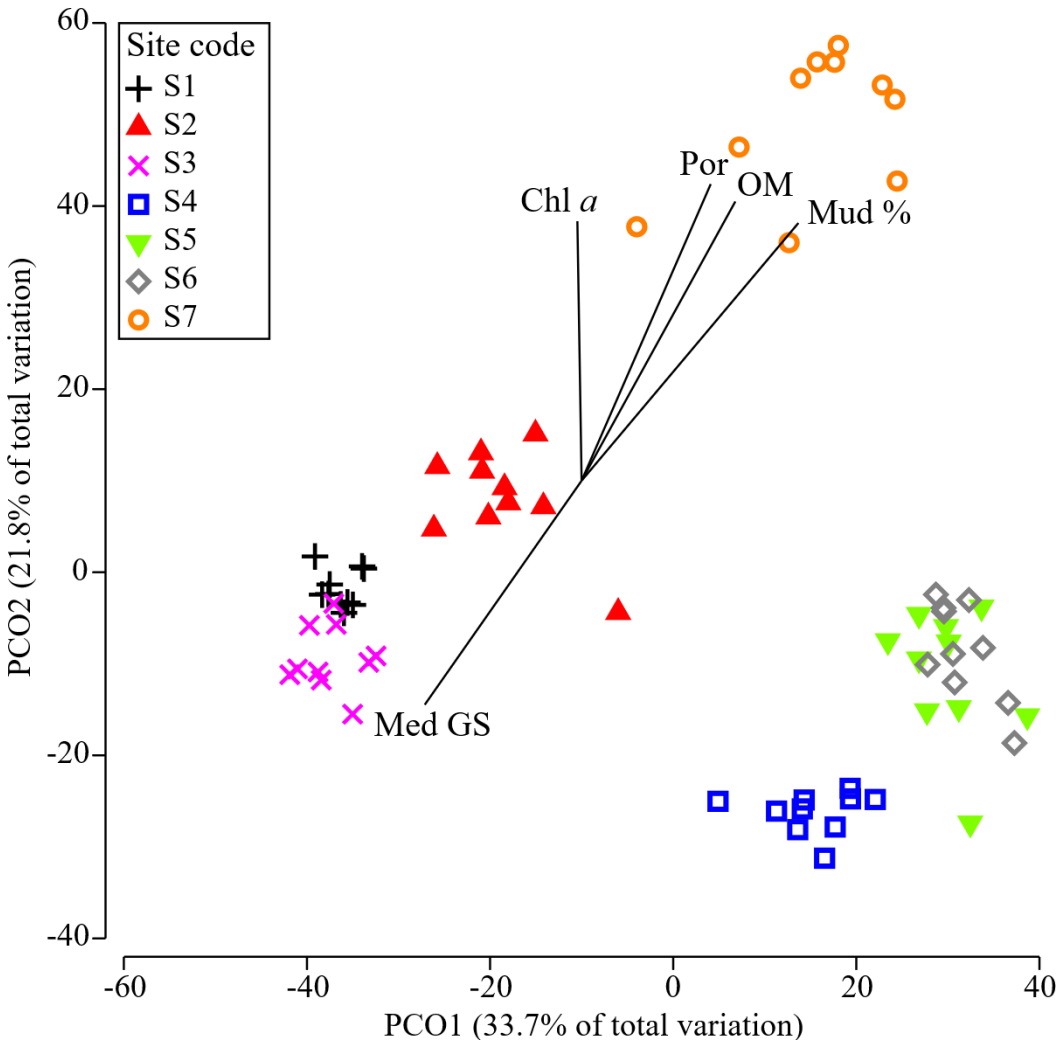

Figure 3.4: Principle coordinate analysis (PCO; using Bray-Curtis resemblance) of square-root transformed community structure at each site (S1 – S7). Vector overlays display the sediment properties that influence community structure.

3.4 Ecosystem functioning

3.4.1 DO fluxes and GPP

Flux chamber incubations showed decreasing net primary production (NPP; light chambers; Table 3.7 and Figure 3.5a) from sites 1 to 7, with a range in average light chamber DO flux values across sites of >7000 µmol O_2 m^{-2} h^{-1}. Light chambers at sites 1-3 exhibited DO production, whereas DO fluxes in light chambers at sites 4-7 were negative or not significantly different from zero (site 5). This indicated a general trend of less net oxygen production and greater oxygen consumption with increasing levels of eutrophication across sites. PERMANOVA analyses (Table 3.8) indicated that overall NPP was significantly different across all sites. In dark chambers, influx of oxygen was observed across all sites, indicating

sediment oxygen consumption (SOC; i.e. negative DO flux). SOC was greatest at site 7, the least at site 4, and unlike NPP, showed no general trend from site 1 to 7. Within site variability was relatively low in Figure 3.5a, indicated by the low standard deviation. PERMANOVA analyses (Table 3.8) indicated that dark chamber SOC was significantly different across all sites. Post-hoc pairwise tests show sites 1 and 5, 2 and 4, and 3 and 7 were not statistically different from each other, while site 6 was distinct from all sites.

Figure 3.5b shows sites 1 to 3 had the highest GPP (GPP = NPP-SOC), ranging from 5020 to 8265 μmol O_2 m^{-2} h^{-1}, and sites 5 to 7 followed a similar trend only at lower production levels (2106 to 3779 μmol O_2 m^{-2} h^{-1}); the minimum GPP was seen at site 4 (406 μmol O_2 m^{-2} h^{-1}). When GPP was normalised by chlorophyll *a* ($GPP_{chl\ a}$ = GPP/chl *a*), there was an order of magnitude decrease across all sites. Site 4 (Figure 3.5c) remained the lowest in $GPP_{chl\ a}$ (42 μmol O_2 m^{-2} h^{-1}), while site 2 became the highest (459 μmol O_2 m^{-2} h^{-1}). Sites with higher *Gracilaria* spp. cover (Table 3.1) decreased in $GPP_{chl\ a}$; for example, site 7 (*Gracilaria* spp. cover 69%) decreased relative to the other sites. The increase in $GPP_{chl\ a}$ (relative to other sites) at site 2, which only had 1 % *Gracilaria* spp. cover, indicates microphytobenthos biomass may be influencing GPP.

3.4.2 **Inorganic nutrient fluxes**

Dark chamber ammonium flux (NH_4^+-N) and dissolved reactive phosphorus flux (PO_4^{3-}-P; Table 3.7; Figure 3.6a and b) showed no general trend across sites, other than both peaking at site 7 (which also displayed the greatest variability in PO_4^{3-}-P flux). NH_4^+-N efflux occurred across all sites, with a range of 76 to 1023 μmol NH_4^+-N m^{-2} h^{-1}, whereas PO_4^{3-}-P showed uptake (influx) at sites 2 and 5. PO_4^{3-}-P efflux at site 7 was 49% greater than the next highest PO_4^{3-}-P efflux (range = 21 to 63 μmol PO_4^{3-}-P m^{-2} h^{-1} across all efflux sites), but was still an order of magnitude lower than NH_4^+-N efflux rates.

PERMANOVA analyses (Table 3.8) indicate that overall, fluxes varied significantly across the sampled gradient, with NH_4^+-N showing significant differences between sites, where sites 1, 3 and 6 were not statistically different from each other. Sites 2, 4 and 5 did not display significant differences in NH_4^+-N flux

rates. For PO_4^{3-}-P, sites 2 and 5 were both significantly distinct from sites 1, 3, 4, and 7. Site 6 was also significantly different to site 7.

Nitrate and nitrite (NO_x-N; Figure 3.6c) was taken up by the sediment at most sites, with fluxes ranging from -652 to 126 μmol NO_x-N m^{-2} h^{-1}. Site 6 had the greatest NO_x-N influx. NO_x-N influxes decreased from sites 1 to 3 and became effluxes at site 4, indicating that site 4 was the only site to not take up NO_x-N from overlying water. Table 3.7 shows NO_x-N had the least significant differences between sites, where site 3 was statistically different from 6, and site 4 was different from 3, 5, 6 and 7.

Table 3.7: Site averaged NPP, SOC and dark chamber nutrient fluxes ± 1 SD; units = μmol m^{-2} h^{-1}.

	Site 1	Site 2	Site 3	Site 4	Site 5	Site 6	Site 7
NPP	2672 (± 876)	3739 (± 1811)	2391 (± 836)	-532 (± 1352)	123 (± 1060)	-692 (± 756)	-3292 (±1665)
SOC	-3814 (± 187)	-1281 (± 283)	-5875 (± 926)	-938 (± 478)	-3656 (± 735)	-2797 (± 494)	-6903 (± 1586)
$GPP_{chl\ a}$	267 (± 33)	274 (± 149)	335 (± 84)	42 (± 99)	293 (± 55)	98 (± 14)	68 (± 47)
NH_4^+-N	397 (± 110)	83 (± 24)	308 (± 38)	181 (± 58)	76 (± 100)	375 (± 125)	1023 (± 284)
PO_4^{3-}-P	21 (± 11)	-2 (± 14)	25 (± 6)	32 (± 7)	-7 (± 12)	2 (± 37)	63 (± 54)
NO_x-N	-164 (± 132)	-150 (± 307)	-65 (± 9)	126 (± 95)	-251 (± 203)	-652 (± 522)	-76 (± 105)

Table 3.8: PERMANOVA test (Euclidian distance resemblance matrix, 999 permutations) on light chamber DO flux (NPP), dark chamber SOC, solute fluxes and $GPP_{chl\ a}$ as a function of site. Pair-wise post-hoc tests show significant differences ($p < 0.05$ shown in bold).

	Source	dF	MS	Pseudo-F	p(perm)	Pair-wise tests
NPP	Site	6	27.56	19.95	**0.001**	1>4, 1>5, 1>6, 1>7, 2>4, 2>5, 2>6, 2>7, 3>4, 3>5, 3>6, 3>7, 4>7, 5>7, 6>7
	Residual	28	6.45			
SOC	Site	6	4.73	33.92	**0.001**	1<2, 1>3, 1<4, 1<6, 1>7, 2>3, 2>5, 2>6, 2>7, 3<4, 3<5, 3<6, 4>5, 4>6, 4>7, 5<6, 5>7, 6>7
	Residual	26	0.14			
$GPP_{chl\ a}$	Site	6	3.79	10.59	**0.001**	1>4, 1>6, 1>7, 2>4, 2>6, 2>7, 3>4, 3>6, 3>7, 4<5, 5>6, 5>7
	Residual	26	0.36			
NH_4^+-N	Site	6	4.63	28.31	**0.001**	1>2, 1>4, 1>5, 1<7, 2<3, 2<4, 2<6, 2<7, 3>4, 3>5, 3<7, 4<6, 4<7, 5<6, 5<7, 6<7
	Residual	26	0.16			
PO_4^{3-}-P	Site	6	2.54	3.93	**0.002**	1>2, 1>5, 2<3, 2<4, 2<7, 3>5, 4>5, 5<7, 6<7
	Residual	26	0.65			
NO_x-N	Site	6	2.58	4.05	**0.008**	3<4, 3>6, 4>5, 4>6, 4>7
	Residual	26	0.64			

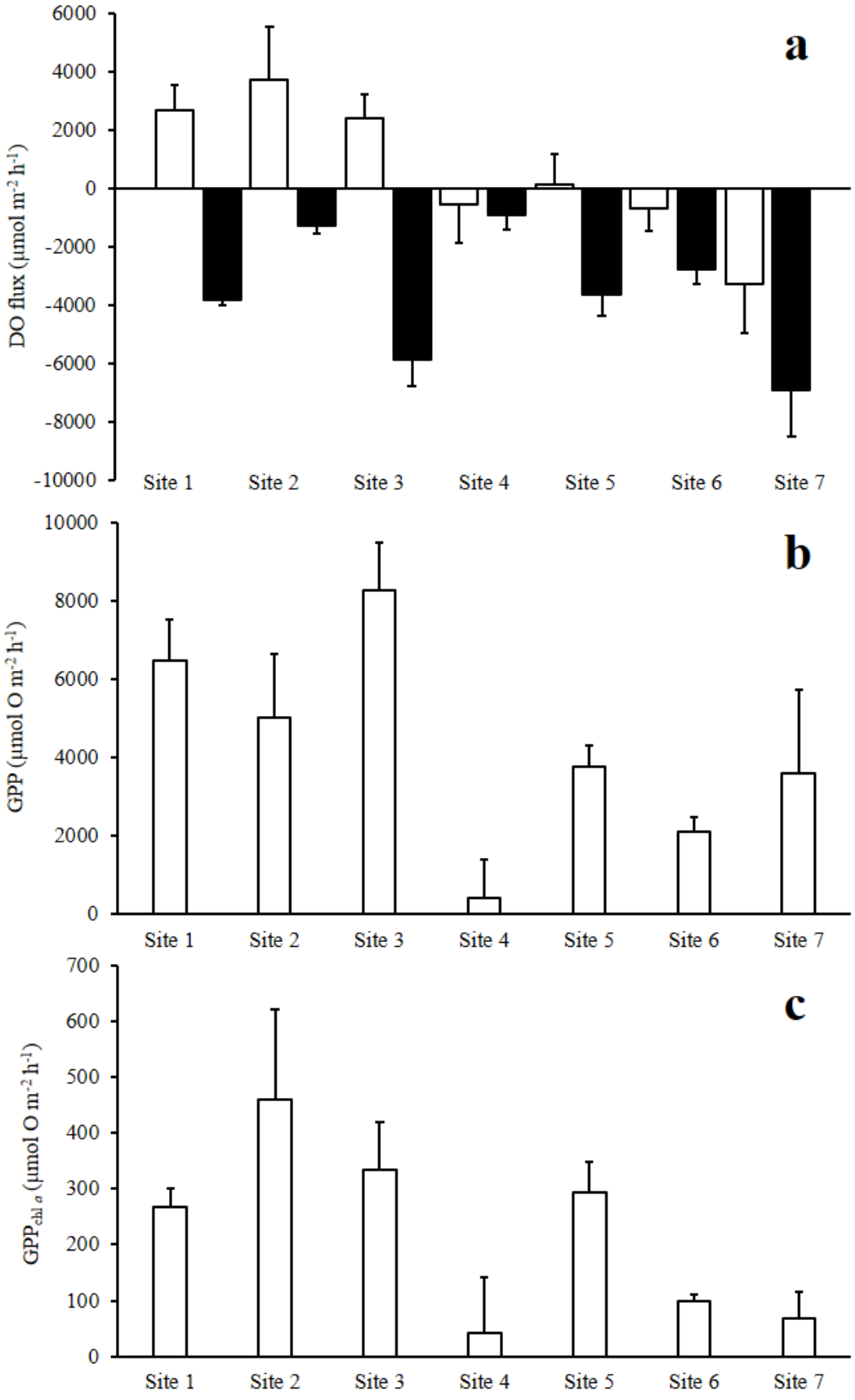

Figure 3.5: Mean (+ SD) of (a) dissolved oxygen flux, where □ = light chambers and ■ = dark chambers, (b) GPP, and (c) $GPP_{chl\ a}$ across all sites. Note the magnitude of change between the y-axes of GPP and $GPP_{chl\ a}$.

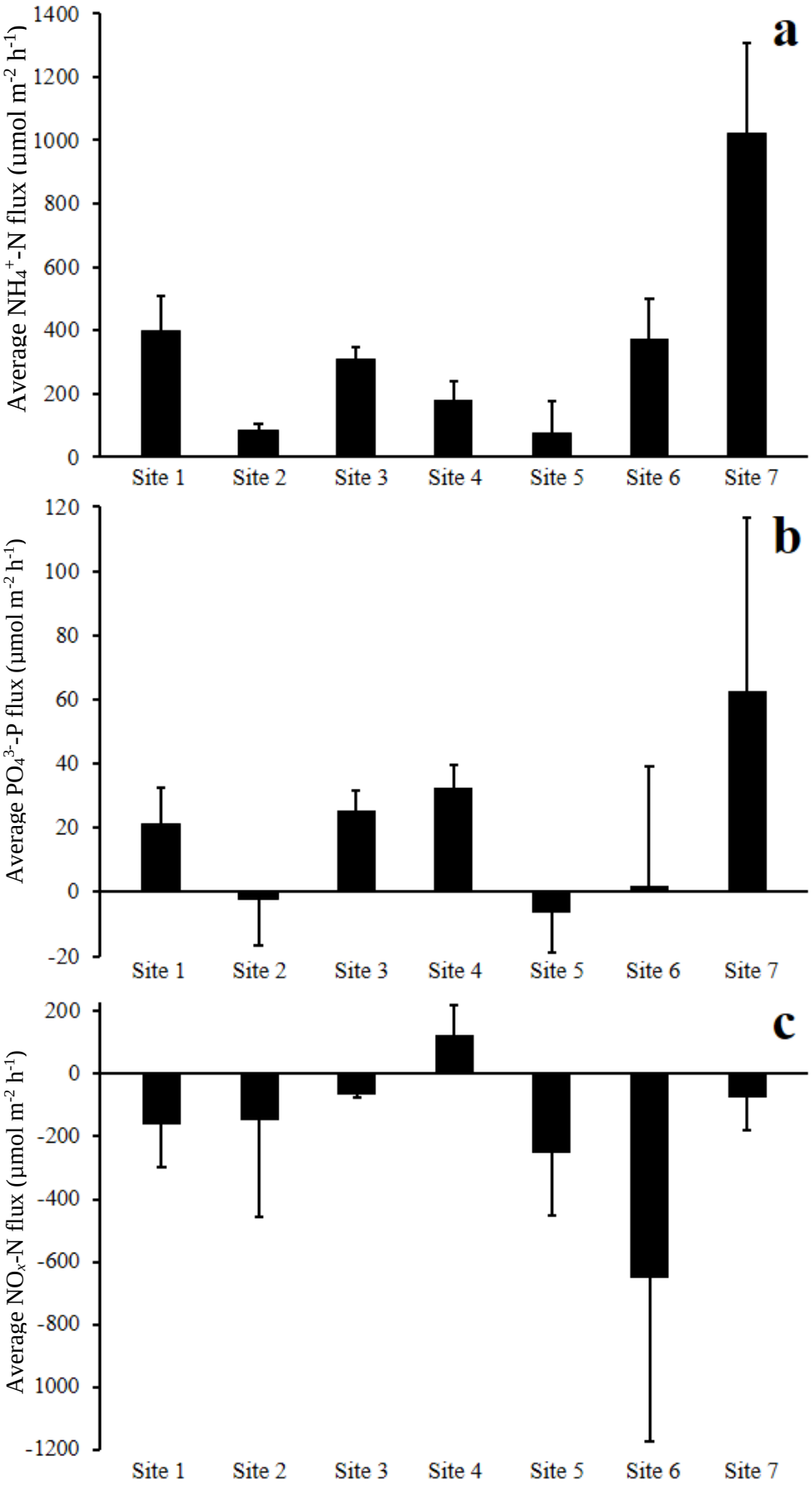

Figure 3.6: Mean (+ SD) of (a) NH_4^+-N flux, (b) PO_4^{3-}-P flux, and (c) NO_x-N flux across all sites, where ■ = dark chambers..

3.5 Ecosystem functioning

To relate biological interactions to ecosystem multifunctionality a principal component analysis was conducted (Figure 3.7a). Multivariate data consisting of dark chamber NH_4^+-N, PO_4^{3-}-P and NO_x-N fluxes was overlain with macrofaunal species vectors (those that explained a substantial proportion of the variance as indicated by SIMPER analysis). PC1 explained 64.5% of the variability in the data, and PC2 explained 31.7%. Species vector overlays varied in length and direction, with *M. liliana* and *Paracorophium* spp. positively correlated to each other and less common at the more eutrophic sites (sites 6 and 7). *Microspio maori*, *Prionospio aucklandica*, *Colurostylis lemurum* and *Ceratonereis* spp. were inversely related to flux data from site 7 and showed little correlation with each other.

Figure 3.7b displays the same multifunctionality ordination as Figure 3.7a, but sediment properties vectors have been overlain. As with Figure 3.4, the direction of mud %, OM and P, were all closely associated and positively correlated with site 7. Med GS was negatively correlated to these variables, pointing towards the less eutrophic sites.

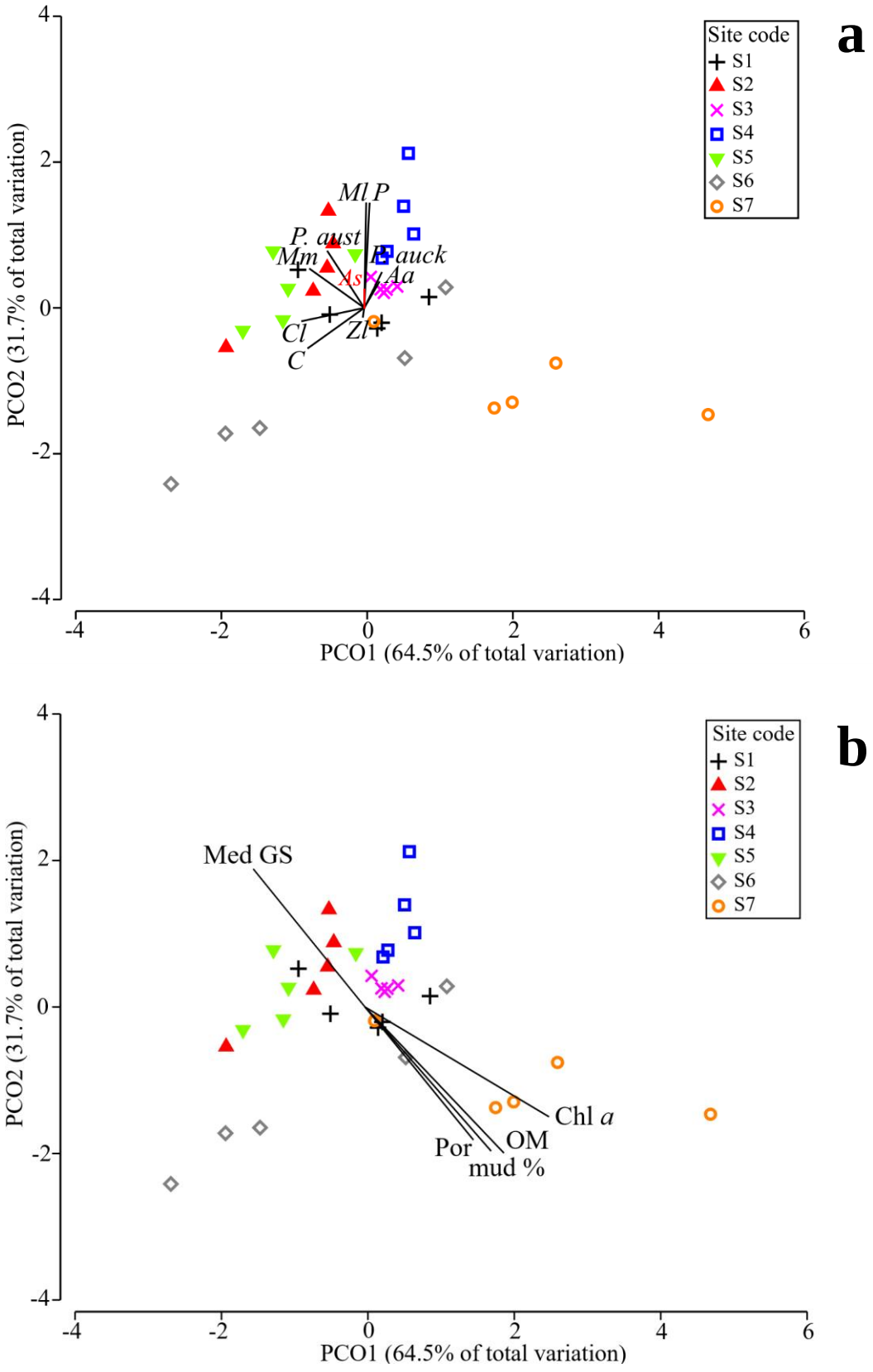

Figure 3.7: Principal component analysis (PCO) of dark chamber fluxes of NH_4^+-N, dissolved reactive phosphorus (PO_4^{3-}-P), and NO_x-N, with vector overlays of (a) 10 species indicated by SIMPER and (b) environmental variables.

3.5.1 **Understanding ecosystem functioning**

Distance based linear models (DistLM) were run to quantify the best environmental and biological predictors of SOC, $GPP_{chl\ a}$ and dark chamber nutrient fluxes. Marginal tests (Table 3.9) show the proportion of variance each explanatory variable contributed irrespective of the other variables measured. In the marginal tests, *Gracilaria* spp. explained the largest amount of variability in SOC (40%), followed by OM (30%). For $GPP_{chl\ a}$, Med GS (Appendix 2) individually explained the most variance (46%), with OM individually explaining 29%. OM and phaeo independently explained NH_4^+-N (72%), reflecting their close correlation (P = 0.83). Phaeo was the largest individual predictor of PO_4^{3-}-P (60%), and *M. liliana* (Appendix 2) was the highest individual explanatory variable of NO_x-N at 11%. In comparison to sediment variables, macrofauna did not explain much of the variance in solute fluxes when treated independently, though *Paracorophium* spp. was relatively high for $GPP_{chl\ a}$ (19%).

DistLM sequential tests (Table 3.10) showed which explanatory variables were significantly influencing SOC, $GPP_{chl\ a}$, and dark chamber nutrient fluxes. To avoid issues of collinearity between OM and mud % (correlation coefficient R = 0.94; Table 3.2), only OM was included in the models. Explanatory variables were retained for use in final models if significant at $p < 0.1$, but p was < 0.05 for most variables. Overall, AICc values were relatively low, and ranged from –6.46 to -66.24, meaning the in-sample fit of explanatory to response variables was relatively close and similar across models.

The most parsimonious SOC model had six explanatory variables and a total explained variance of 83% (adjusted R^2), with OM explaining 35% of the total. Sediment chl *a* contributed almost equally to that of OM for SOC (34% of the R^2), though chl *a* showed an inverse relationship to OM; as chl *a* increased so did SOC. Macrofauna explanatory variables retained in the model had a positive correlation with SOC, that is, increases in *Paracorophium* spp. and *M. liliana* abundance were associated with an increase in SOC. The larger *M. liliana* (>10 mm) explained more than twice the amount of variation in SOC than the smaller *M. liliana* (<10 mm). The most parsimonious $GPP_{chl\ a}$ model accounted for 53% of the variance (adjusted R^2), and was explained equally by two variables; OM and *Paracorophium* spp. Both OM and *Paracorophium* spp. were negatively correlated

to $GPP_{chl\ a}$, indicating that a decrease in these two variables is related to a decrease in $GPP_{chl\ a}$.

Three explanatory variables explained 89% (adjusted R^2) of the variation in NH_4^+-N flux, with OM explaining 80.6% of the R^2, followed by phaeo at 12.6%. Macrofauna, namely *A. stutchburyi* (adult and juvenile), explained the remaining 6.8% of the model variance. Increases in OM and phaeo were associated with increased NH_4^+-N fluxes (i.e. positive correlation), while *A. stutchburyi* were negatively associated with NH_4^+-N fluxes. The most parsimonious PO_4^{3-}-P model explained a total of 73% (adjusted R^2) of the variation in PO_4^{3-}-P flux. PO_4^{3-}-P flux was primarily explained by differences in phaeo pigment concentration (47%), accounting for half of the explained variance, followed by OM and aRPD depth (35 and 15% respectively). As with NH_4^+-N, a smaller portion of the variance in PO_4^{3-}-P flux was explained by macrofauna – in this case *A. stutchburyi* (5%). These three explanatory variables were all positively correlated to PO_4^{3-}-P flux.

The model with the least variability explained (32%; adjusted R^2) was for NO_x-N flux, which differed from the other fluxes, being driven by aRPD, chl *a* and *Ceratonereis* spp., not by OM. aRPD depth and chl *a* were positively correlated with NO_x-N fluxes, indicating that an increase in NO_x-N flux is associated with an increase in aRPD depth and chl *a*, while *Ceratonereis* spp. are negatively correlated to NO_x-N fluxes.

Table 3.9: DistLM marginal tests for response variables included in sequential tests of SOC, $GPP_{chl\ a}$, dark chamber NH_4^+-N, dark chamber PO_4^{3-}-P and dark chamber NO_x-N. For all other response variables see Appendix 2.

	Variable	SS(trace)	Pseudo-F	P	Prop.
SOC					
	OM	9.70	13.49	<0.01	0.30
	Chl *a*	0.29	0.28	0.60	0.01
	Gracilaria spp.	12.82	20.72	<0.01	0.40
	Paracorophium spp.	2.05	2.13	0.14	0.06
	M. liliana <10 mm	0.02	0.02	0.89	<0.01
	M. liliana >10 mm	0.51	0.50	0.50	0.02
$GPP_{chl\ a}$					
	OM	9.34	12.77	<0.01	0.29
	Paracorophium spp.	5.93	7.05	0.01	0.19
NH_4^+-N					
	OM	23.09	80.38	<0.01	0.72
	Phaeo	23.17	81.30	<0.01	0.72
	Total *A. stutchburyi*	0.01	0.01	0.95	<0.01
PO_4^{3-}-P					
	OM	7.96	10.27	0.01	0.25
	Phaeo	19.24	46.72	<0.01	0.60
	aRPD	1.74	1.78	0.20	0.05
	Total *A. stutchburyi*	0.07	0.07	0.78	<0.01
NO_x-N					
	OM	0.16	0.15	0.69	<0.01
	Chl *a*	2.41	2.52	0.13	0.08
	aRPD	2.19	2.28	0.14	0.07
	Ceratonereis spp.	2.85	3.03	0.09	0.09

Table 3.10: DistLM sequential tests for response flux variables of SOC, $GPP_{chl\ a}$, dark chamber NH_4^+-N, dark chamber PO_4^{3-}-P and dark chamber NO_x-N. Also displayed is the percentage of the R^2 explained by given explanatory variables, and the correlation direction of explanatory variables in relation to response variables (+ or -). Explanatory variable significance levels were all $p<0.1$, but most often $p<0.05$.

	Explanatory variables	Sequential test prop.	% of R^2 explained	Correlation direction
SOC				
Sediment	OM	0.30	35.29	-
	Chl *a*	0.30	34.72	+
	Gracilaria spp.	0.06	7.13	-
Macrofauna	*Paracorophium* spp.	0.05	5.50	+
	M. liliana>10 mm	0.10	11.85	+
	M. liliana<10 mm	0.05	5.51	+
	R^2	0.86		
	Adjusted R^2	0.83		
	AICc	-47.20		
$GPP_{chl\ a}$				
Sediment	OM	0.29	48.82	-
Macrofauna	*Paracorophium* spp.	0.31	51.18	-
	R^2	0.60		
	Adjusted R^2	0.57		
	AICc	-24.23		
NH_4^+-N				
Sediment	OM	0.72	80.56	+
	Phaeo	0.11	12.62	+
Macrofauna	Total *A. stutchburyi*	0.06	6.83	-
	R^2	0.90		
	Adjusted R^2	0.89		
	AICc	-66.24		
PO_4^{3-}-P				
Sediment	OM	0.25	34.64	+
	Phaeo	0.36	50.44	+
	aRPD	0.11	14.92	-
Macrofauna	Total *A. stutchburyi*	0.04	5.32	+
	R^2	0.76		
	Adjusted R^2	0.73		
	AICc	-35.93		
NO_x-N				
Sediment	OM	0.005	1.22	-
	Chl *a*	0.13	31.32	+
	aRPD	0.19	47.07	+
Macrofauna	*Ceratonereis* spp.	0.08	20.39	-
	R^2	0.40		
	Adjusted R^2	0.32		
	AICc	-6.46		

Chapter Four

Discussion

Waihī Estuary has been subjected to large amounts of anthropogenic terrestrial sedimentation, organic matter (OM) and nutrient inputs particularly for the last 90 years (since canal channelising), which has resulted in eutrophication, predominantly in the upper reaches of the estuary. Waihī Estuary showed clear evidence of eutrophic symptoms, which provided a gradient of change from relatively un-impacted to degraded habitats within the system. This study used an *in-situ* eutrophication gradient and measured the sediment environment, macrofaunal community and ecosystem functioning (solute fluxes) to answer the following questions:

- How does the sediment environment vary across the gradient and how does this alter the macrofaunal community structure?
- How do the small-scale drivers of ecosystem function change along the gradient and what drives site level change?
- How does eutrophication alter ecosystem function at a system wide scale and what interactions and drivers are responsible for the resultant outcome?

4.1 Physical changes across the eutrophication gradient

Mud content (mud %; defined as grain sizes < 63 μm) and OM were highly correlated within the estuary (Table 3.2), which is consistent with other eutrophication studies (De Falco *et al.*, 2004; Pratt *et al.*, 2014a; Douglas *et al.*, 2018). This high correlation is likely a consequence of multiple interacting factors. Firstly, fine sediments (along with OM and inorganic nutrients), are inputted from rivers (Bricker *et al.*, 2008; Tay *et al.*, 2013). In Waihī Estuary, the canals empty into the upper reaches of the estuary, where near-bed tidal flows, surface wave action and water depth appear lower compared to the well flushed areas near the estuary mouth. This creates a settling lag, whereby particles are preferentially settled onto the sediment surface when the water currents can no longer hold the relative grain sizes in suspension (Green & Coco, 2014). Secondly, because

muddier sediments have a higher surface area per volume ratio (compared to coarser sediments), there is a greater surface for bacteria to grow on (Arndt *et al.*, 2013).

Waihī Estuary had the highest OM and mud content (%) at the site closest to riverine inputs (site 7): 8.3% and 90.5% respectively, which is comparatively high relative to other North Island, New Zealand estuaries (Pratt *et al.*, 2014a). Increases in chlorophyll *a* (chl *a*) and phaeophytin (phaeo) concentrations were associated with increasing *Gracilaria* spp. cover (Table 3.2). This is likely because *Gracilaria* spp. itself is a photosynthetic organism, thus containing chl *a* pigment and upon degradation, phaeopigment (Guillemin *et al.*, 2014; Nelson *et al.*, 2015).

In this study, increased median grain size (Med GS) was correlated with reductions in porosity and increased fine sediments (Table 3.2), which is consistent with measurements taken in other NZ estuaries (Norkko *et al.*, 2002; Needham *et al.*, 2011; Lohrer *et al.*, 2013). Spinelli *et al.* (2004) reviews that grain size, grain shape and packing are parameters that effect unconsolidated sediment porosity. In general, given a relatively uniform grain size, finer sediments, such as those seen at the upper reaches of Waihī Estuary, have a higher porosity because of the interstitial void space between the fine particles (Spinelli *et al.*, 2004). Higher porosities are often associated with higher nutrient concentrations within sediments through greater pore water retention. Furthermore, the addition of fine sediments creates a diffusive rather than advective environment (Janssen *et al.*, 2005). This, along with complex biological interactions, influences the rate of solute exchange to and from the sediment surface (Huettel & Gust, 1992).

4.2 Environment and macrofauna

As OM content increased along the eutrophication gradient, an overall decrease in the taxonomic richness of macrofauna became evident (Table 3.4). Effects on community structure were also identified (Figure 3.1). If OM input exceeds what the heterotrophic benthic community can aerobically process (often associated with summer algal blooms), then the system may periodically become hypoxic (Diaz & Rosenberg, 2008). Hypoxic waters have been shown to negatively influence community structure through migration, decreased efficiency and mortality (Marsden & Bressington, 2009; Lewis & DeWitt, 2017). Furthermore, the input of fine sediments can reduce the presence of filter feeders as smaller particles reduce

feeding efficiencies (Jones, 2011). Therefore, species that are less tolerant to increased eutrophication, have narrower lower and upper limits to the ecological niche in which they can survive (Hewitt *et al.*, 2008). For example, *Austrovenus stutchburyi* plays key bioturbational and water filtering roles in NZ estuaries (Jones, 2011; Lohrer *et al.*, 2016). They are a highly mobile suspension feeding bivalves that bulldoze through surficial sediments (Thrush *et al.*, 2006). Being suspension feeders, increased levels of fine suspended sediment can clog and damage their filter feeding structures, decrease the quality of seston (particulate suspended matter) that is used for nutrition and therefore limit their distribution (Cheung & Shin, 2005). In this study, *A. stutchburyi* declined where there was a 10% increase in mud content between sites 3 and 4 (Figure 3.1; Appendix 1, Table A.1). This is consistent with the findings of Anderson (2008) and Norkko *et al.* (2006) who showed that *A. stutchburyi* are tolerant to lower levels of mud than other bioturbating species (optimum 11% mud) and are sensitive to repeated high exposure of fine suspended sediment.

Taxonomic richness across all the sites showed a relatively linear decrease (Figure 3.2), which is consistent with the findings of Pratt *et al.* (2014a), but differed slightly from Pearson and Rosenberg (1978) who noted an increase in taxonomic richness with a slightly elevated OM content, as organisms need organic matter (i.e. food) to survive. This phenomena is not seen in the current study, most likely because site 1 (having the lowest OM content of 2.3%) was already past point of initial OM enrichment described by Pearson and Rosenberg (1978) which ranged from 2.2 to 3.1% OM.

Patterns in species abundance followed the Pearson and Rosenberg (1978) model, where biomass decreased to the transitional sharp increase in abundance of opportunistic species followed by a rapid decline (Figure 3.2). In this study, *Paracorophium* spp. dominated in number at site 4 and was also present in high densities at sites 5 and 6 (Figure 3.3). These suspension feeding amphipods fulfil similar functions to the better researched *Corophium volutator* and *Corophium insidiosum* (Henriksen *et al.*, 1983; Pelegri & Blackburn, 1994; Moller & Riisgard, 2006). Meadows (1964), suggested that *C. volutator* prefers muddier fine sand; conditions that match those of site 4. Site 4 had the combination of muddier fine sands and consequently a lower taxonomic richness (particularly the

reduction of *A. stutchburyi* and the loss of the larger *Macomona liliana*), which provided ideal conditions for *Paracorophium* spp. to proliferate. Pearson and Rosenberg (1978) noted that upon further progression of OM input, this opportunistic species also rapidly declined, as they have a narrow distribution range. Such was the pattern between sites 4 and 5, where *Paracorophium* spp. abundance declined by over 70%.

As OM enrichment progressed to site 6, juvenile *M. liliana* were lost, as were *Prionospio aucklandica*. However, certain polychaetes increased in abundance. *Capitella sp*. have an optimum mud content range of 10 to 40%, can tolerate up to 95% mud content and thrive in highly organically enriched sediment (Tsutsumi, 1990). *Capitella sp*. are therefore used as indicators of stressed and disturbed environments (Dean, 2008). The two-fold shift in the amount of OM content and mud % from site 5 to 6 and the concurrent increase in *Capitella sp*. is consistent with literature, as *Capitella sp*. are opportunistic and require organically enriched sediment for normal growth (Tsutsumi, 1990). As OM enrichment further increases, *Capitella sp*. abundance declines, which agrees with the current study, where *Capitella sp*., decreased from site 6 to 7 (Appendix 1, Table A.1).

Another key bioturbating species found in this study was the tellinid bivalve *M. liliana*. Juvenile *M. liliana* (shell length < 10 mm), are limited to the upper 2 cm of sediment and have shown to move within sediment and the water column (Cummings *et al.*, 1993, 1995; Hewitt *et al.*, 1997). Adult *M. liliana* (shell length > 10 mm) live deeper in the anoxic sediment layers, deposit feeding on the microbial biomass at the sediment surface via a long inhalant siphon and subsequently excreting at depth (Hewitt *et al.*, 1997). Therefore, juvenile and adult *M. liliana* perform different functions within the sediment (Cummings *et al.*, 1993; Hewitt *et al.*, 1997). In the current study, adult *M. liliana* were seen in mud concentrations of 3.6 to 8.7% (sites 1 to 3), which is a lower than that observed by Anderson (2008) who reports that *M. liliana* have a higher preferred mud content than *A. stutchburyi* (17%). *M. liliana* have been shown to be sensitive to the effect of eutrophication, with deposits of fine sediment influencing feeding rates and the degree of pore water pressurisation (McCartain *et al.*, 2017). Beyond site 3, there was also a 50% reduction in chl *a* content at sites 4 to 5 (Table 3.1), indicating that adult *M. liliana* may have also lost an important food source.

Macrofaunal feeding activities and structures in the sediment can influence the apparent redox potential discontinuity (aRPD) depth, increasing the surface area available for solute exchange. Burrow linings can become sites of high metabolic and microbial activity compared to the surrounding sediment (Crawshaw *et al.*, 2019). Therefore, a reduction in abundance and species diversity (if key functional traits are lost) can alter the sediment mosaic, influencing OM recycling by altering the redox profile.

4.2.1 **Redox environment**

There are a diverse range of microorganisms that utilise a variety of electron acceptors to oxidise OM in marine sediments (Jørgensen, 1977b; Sørensen & Revsbech, 1979; Henrichs & Reeburgh, 1987; Canfield *et al.*, 1993; Rysgaard *et al.*, 1994). Being the most favourable and abundant electron acceptor, oxygen (if present) is generally rapidly depleted in the upper millimetres of sediment (Glud, 2008). In a lot of environments, the degradation of benthic carbon is thus mediated by microbes anaerobically using nitrate, manganese oxides, iron oxides and/or sulphate electron acceptors (Fenchel *et al.*, 2012). Methanogenesis can further degrade organic carbon in the absence of these oxidants, but according to Froelich *et al.* (1979) this process does not represent the net oxidation of organic carbon. Sediments will typically show a vertical redox zonation where electron acceptors are depleted sequentially in the order outlined above, indicating the potential energetic gain related to the particular redox process (Fenchel *et al.*, 2012). Products that are reduced from anaerobic degradation can be re-oxidised by oxygen via direct means or through complex microbially catalysed redox cascades (Fenchel *et al.*, 2012).

The bioturbation of benthic fauna creates a heterogeneous landscape, where the rates of processes over the area-integrated vertical profile can result in overlapping zonation of heterotrophic pathways (Canfield *et al.*, 1993). The loss of bioturbators due to stressors such as eutrophication, sedimentation and hypoxia, can reduce aRPD depth, which in turn can alter the sediment dynamics and macrofaunal functions (Kristensen, 1988). Therefore, the different oxidation pathways are governed by bioturbation and sedimentation rates and the water and sediment chemistry.

In the current study, OM ranged by 0.6% from sites 1 to 5, however, there was an almost two-fold increase in OM from site 5 to site 6, and a three-fold increase from site 5 to site 7 (Table 3.1). The heterotrophic organisms are unable to entirely utilise the labile OM or rework it into deeper sediments at site 6 and 7 before the onset of hypoxia, shown by the large influxes of DO at these sites (Herbert, 1999). Aerobic respiration in these surface sediments rapidly depletes, reducing aRPD depth. Alternative electron acceptors (highlighted above) are then sequentially used as oxidants in microbial anaerobic respiration (Kerner, 1993), ultimately leading to toxic hydrogen sulphide (H_2S) production. H_2S can also be precipitated from metal ions in the sediment, but this pathway represents only a small portion of production (Middelburg & Levin, 2009).

Gracilaria spp. cover can also induce periods of anoxia, subsequent reduction in aRPD depth and the development of hydrogen sulphide as the consequence of anaerobic OM decomposition (Hale *et al.*, 2016). Where highest *Gracilaria* spp. cover was observed (site 7), *Beggiatoa* spp., a filamentous bacteria that lives at the transition zone between oxygen and H_2S (Jørgensen & Revsbech, 1983), formed visible surface patches. *Beggiatoa* spp. can anaerobically reduce sulphide, influencing production (Jørgensen, 1977a; Jørgensen & Revsbech, 1983). It is unlikely that site 7 had completely reduced to toxic sulphidic conditions, as macrofaunal organisms were still present (albeit in reduced numbers and diversity), namely species tolerant to highly eutrophic conditions, e.g. *Potamopyrgus estuarine* and *Oligochaeta* spp.

4.3 Site specific changes in function

Examining site specific changes in ecosystem functioning provides an important measure of the finer scale processes, which can give greater resolution to why and how changes are occurring across the entire eutrophication gradient (Hewitt *et al.*, 2007). Net primary production (NPP) generally decreased across all sites, with the exception of sites 1 and 3, while sediment oxygen consumption (SOC) showed no general trend other than being most negative at site 7 (Table 3.7; Figure 3.5a). OM enrichment and hypoxia strongly influence the fluxes of dissolved oxygen (DO), ammoniacal nitrogen (NH_4^+-N), dissolved reactive phosphorus (PO_4^{3-}-P) and nitrate and nitrite (in combination, NO_x-N), but different processes can result in

efflux or influx of solutes at the sediment-water interface (Hale *et al.*, 2016). Therefore, the supply of OM and the availability of oxygen are key factors that govern nutrient recycling (Glud, 2008; Meyer *et al.*, 2015). In the current study, at the less impacted end of the gradient, light chamber NPP was in efflux, and as the gradient increased, there was a switch where the system's oxygen demand outweighed microphytobenthos oxygen production (Figure 3.5a).

4.3.1 **Patterns in dissolved oxygen and gross primary productivity**

DO fluxes are linked between the balance of oxygen production from microphytobenthos (MPB) and oxygen consumption from the respiring macrofaunal community (Glud, 2008). The least impacted site, site 1, had the greatest number of *Austrovenus stutchburyi*, lower NPP and greater SOC than site 2 (Figure 3.5a). This result is consistent with that of Sandwell *et al.* (2009), who manipulated the *in-situ* density of adult *A. stutchburyi* (from 20 to 2000 ind. m^{-2}). Sandwell *et al.* (2009) found an almost three-fold increase in SOC in light and dark chambers due to the increased demand for oxygen via respiration. The densities of *A. stutchburyi* in the current study (based on the upscaling of ten 0.013 m^{-2} macrofauna cores per site) were 6,720 and 360 individuals m^{-2} (site 1 and 2 respectively). However, it is important to note, that while I observed greater densities, 98% of these organisms were juveniles (<10 mm shell length). Between site 1 and site 2 there was an almost three-fold reduction in the rate of dark chamber SOC (Figure 3.5a), which is almost exactly that of Sandwell *et al.* (2009) despite the greater abundance of *A. stutchburyi* we observed in the current study. This result highlights the differences between the effects of juvenile and adult *A. stutchburyi*, where the respiration of abundant juveniles is substantially less than respiration of fewer adults (Peters, 1983; Norkko *et al.*, 2013).

Thrush *et al.* (2006) found that removing *A. stutchburyi* from an otherwise undisturbed sand flat with a similar grain size increased microphytobenthic biomass. This is because *A. stutchburyi* bulldozes through the surface sediment layers preventing biofilm establishment. However, this was not observed in the current study, where chl *a* content and *A. stutchburyi* both decreased from site 1 to site 2. These results better agree with Jones (2011) and Sandwell *et al.* (2009) who found an increase in MPB (indicated by chl *a* content) with an increase in *A. stutchburyi*

density. Thrush *et al.* (2006) also demonstrated that the removal of large *M. liliana* resulted in the decrease of MPB standing stock, which is consistent with the current study, where after site 3, *M. liliana* were absent and chl *a* decreased by 50% (Figure 3.3; Table 3.1). When GPP was normalised by chl *a*, this resulted in an increase in site 2 $GPP_{chl\ a}$ relative to sites 1 and 3 (Figure 3.5 a and b); indicating an increased photosynthetic efficiency rather than biomass, possibly linked to light conditions on the sampled days. While site 2 was taxonomically as rich as site 1 (Table 3.4), fewer individual organisms were present, which was reflected in the higher light chamber NPP (Figure 3.5a), as there a fewer organisms to consume oxygen. Although this was not measured, there could be an additional influence of macrofaunal biomass, as larger organisms respire at a greater rate than smaller organisms (Hewitt *et al.*, 1997).

Relevant to this section are the processes that alter the aRPD depth (see section 4.2.1). Site 4, where there was a step up in the eutrophication gradient, showed sediment oxygen influx in both light and dark chambers (Figure 3.5a), likely due to the increased *Paracorophium* spp. density. These organisms construct U-shaped burrows in the sediment (i.e. burrows that start and end at the sediment-water interface) and encourage the drawdown of oxygen through constant burrow ventilation using their pleopods (Moller & Riisgard, 2006). The related genus *Corophium* have a large burrow size relative to biomass, further encouraging high irrigation activity (Henriksen *et al.*, 1983). Pelegri and Blackburn (1994) report the burrowing depth of *C. volutator* to be between 20 to 60 mm in depth, which is within the range of oxygen penetration at site 4 of up to 31 mm (Table 3.1). A study by Pelegri *et al.* (1994) established a gradient of 0 to 19,800 *C. volutator* m^{-2} (comparable to the 18,770 *Paracorophium* spp. m^{-2} at site 4), and found that DO uptake doubled across this gradient due to the mass transfer and pumping of water. The oxygen consumption partially derives from *C. volutator* respiration during this continuous activity (Pelegri & Blackburn, 1994). Site 4 had half the amount of MPB compared to sites 1 to 3, combined with the large abundance of respiring *Paracorophium* spp., but also had the deepest aRPD depth (Table 3.1). This is unusual given areas of deeper aRPD depth are generally associated with more productive sediments (Hale *et al.*, 2016; Douglas *et al.*, 2018).

Nitrification in sediments is an aerobic process that can consume a significant quantity of DO in the sediments and influence the balance between anaerobic and aerobic heterotrophy (Henriksen & Kemp, 1988). *Paracorophium* spp. may be fuelling this process and will be discussed in section 4.3.2.3.

4.3.2 Patterns in nutrient fluxes

Three nutrient species were measured as part of this study: namely ammoniacal nitrogen (NH_4^+-N), dissolved reactive phosphorus (PO_4^{3-}-P), and nitrate-plus-nitrite (NO_x-N). Ammoniacal nitrogen encompasses two forms of nitrogen (ammonia; NH_3, and ammonium; NH_4^+) and is the most readily utilised nitrogen species globally in terrestrial, freshwater and marine domains (Stief, 2013). NH_4^+-N can derive from direct land use runoff, but also from the rapid ammonification of particulate organic nitrogen within oxic and anoxic layers of sediment (Stief, 2013). PO_4^{3-}-P represents the pool of dissolved reactive phosphorus which is essential for algal growth. In oxic sediments, PO_4^{3-}-P is bound to iron oxides, however when iron oxides are reduced under anoxic conditions, PO_4^{3-}-P can be released from the sediments (Levin *et al.*, 2009). NO_x-N (nitrite; NO_2^-, and nitrate; NO_3^-) is a highly soluble molecule that derives from the leaching of soil into waterways, but can be produced through the oxidation of ammonium through nitrifying bacteria (Stief, 2013).

4.3.2.1 *Ammoniacal nitrogen*

Although no clear pattern in NH_4^+-N flux was noted between sites (Figure 3.6a), each site showed a flux from the sediment to the overlying water column. Given the differences in community structure and abundance/presence of differing key bioturbating species, this non-linear pattern is unsurprising. For example, Site 1 had the greatest density of *A. stutchburyi* and the largest NH_4^+-N efflux across sites 1 to 5 (Figure 3.6a). Sandwell *et al.* (2009) noted a 5.9 to 6.9 times increase in NH_4^+-N efflux with an increase in *A. stutchburyi* densities. In the current study, between sites 1 and 2 there was a 4.8 times increase in dark chamber NH_4^+-N efflux (Table 3.7), which is slightly lower than that of Sandwell *et al.* (2009). This increase is primarily through excretion and indirectly by depositing organic rich faeces and pseudofaeces (Sandwell *et al.*, 2009). Biodeposits (faeces and pseudofaeces) are organic rich particles and sites of high microbial activity that can

affect the distribution of solutes in surrounding sediments (Kristensen, 1988). Biodeposits from suspension feeding clams, particularly influence the oxic environment, as this is where excretion occurs, compared to deposit feeders that excrete at depth (Thrush *et al.*, 2006). The reduction in species abundance at site 2 (50% lower compared to site 1; Figure 3.3) likely contributed to a reduction in NH_4^+-N efflux. These results are contrary to Thrush *et al.* (2006), who found that the removal of *A. stutchburyi* had no impact on NH_4^+-N and DO in dark chambers.

Hale *et al.* (2016) recognised that a feedback loop is created where *Gracilaria* spp. periodically smothers the sediment, causing low DO levels or anoxic conditions (Levin *et al.,* 2009). In low DO conditions, coupled nitrification-denitrification reactions can be inhibited, which increase the NH_4^+-N efflux, in turn fuelling phytoplankton growth (Middelburg & Levin, 2009). If the quantity, quality and spatial distribution of OM (in this case *Gracilaria* spp.) regulates benthic nutrient fluxes (Herbert, 1999), then due to the high content and deposition of OM at site 6 and 7 (Table 3.1), there may have been a shift in the dynamics of solute fluxes (Figure 3.6). Anoxia and decomposition of *Gracilaria* spp., other organic matter and the subsequent decomposition of macrofauna, is likely influencing the NH_4^+-N efflux, which was highest at site 7 (Figure 3.6a). Hale *et al.* (2016) found that in hypoxic areas, ammonium was released into the overlying water column at a rate two to three times faster than in the corresponding oxygenated sediments. These results agree with the current study, where NH_4^+-N efflux at site 7 was 2.6 times greater than the next highest efflux from oxygenated sediment (site 1) (Table 3.7).

4.3.2.2 *Phosphorous*

Hale *et al.* (2016) demonstrated that in hypoxic conditions PO_4^{3-}-P efflux followed NH_4^+-N with a two to threefold increase. This also relates to my findings where PO_4^{3-}-P efflux was two times greater at site 7 compared to the next highest PO_4^{3-}-P efflux at site 4 (Figure 3.6b). When sediments are oxygenated, PO_4^{3-}-P is tightly bound to iron oxides, but under anoxic conditions, PO_4^{3-}-P is reduced and can be rapidly released to the water column, as seen at site 7 (Middelburg & Levin, 2009). However, PO_4^{3-}-P was released from sediments at all sites with the exception of sites 2 and 5 (Figure 3.6b). The oxygenation of sediment from macrofaunal

bioturbation therefore influences PO_4^{3-}-P retention, as PO_4^{3-}-P is readily absorbed to ferric iron in oxic pore waters (Karlson *et al.*, 2007).

4.3.2.3 *Nitrate and nitrite*

Only site 4 demonstrated a net efflux of NO_x-N (Figure 3.6c), with all other sites showing uptake of NOx-N to some degree. The high density of burrow building *Paracorophium* spp. at site 4 provided greater surface area and burrow ventilation. The relatively low NH_4^+-N (Fig 3.6a) flux indicate ammonification and subsequent nitrification (NO_x-N release). These results are consistent with Henriksen *et al.* (1983); Pelegri and Blackburn (1994); Moraes *et al.* (2018) who found that high densities of *Corophium* spp. (a functionally similar genus), increased the flux of NO_3^- to the water column through facilitating nitrification.

The burrow walls of *C. volutator* have shown significantly higher potential nitrification rates than the corresponding oxic sediment layer (Henriksen *et al.*, 1983). Because of the U-shaped burrows and irrigation behaviour, bottom water containing dissolved NH_4^+-N is continuously pumped through the burrows to areas where NO_x-N and O_2 electron acceptors are typically depleted (Kristensen, 2000). Nitrification is thus promoted and NO_x-N that does not undergo reduction or denitrification is flushed into the water column, increasing the NO_x-N flux and decreasing the NH_4^+-N flux as NH_4^+-N is sequestered via nitrification. The lower flux of NH_4^+-N at site 4 is also consistent with the static experiments of Biles *et al.* (2002), as suspension feeders reduce the particulate matter in the water column, which decreases the organic matter available to microbes, reducing ammonification. However, Emmerson *et al.* (2001) also showed that increasing densities of *C. volutator* can increase NH_4^+-N flux rates.

At site 6, the greatest influx of NO_x-N was observed (Figure 3.6c). This influx may be for the purpose of anaerobic microbial nitrate oxidation to manganese in order to further complete the degradation of OM. Also potentially contributing to the influx of NO_x-N at site 6 is the dissimilatory nitrate reduction to ammonium pathway (DNRA), which can occur in anoxic sediments, and converts NO_3^- to NO_2^- and then NO_2^- to NH_4^+ (McCarthy *et al.*, 2008). In anoxic environments, DNRA inhibits denitrification, which could explain the large influx of NO_x-N at site 6. This

has implications for site 7, which had the highest organic content, and contrary to site 6, had the lowest NO_x-N influx and a high NH_4^+-N.

In a study by Kamp *et al.* (2011) on the diatom *Amphora coffeaeformis*, they show that in dark and anoxic conditions, *A. coffeaeformis* consumes NO_3^- and produces NH_4^+, while in light and oxic conditions, NH_4^+ was not produced. This demonstrates that diatoms in the dark and anoxic environment not only act to store NO_3^-, but also facilitate DNRA through their storage of NO_3^- (Kamp *et al.*, 2011). This research supports the hypothesis that at site 7, where *Gracilaria* spp. prevents light penetration and hypoxia is frequent, diatoms may be using their stores of NO_3^-, which is reflected in a low NO_x-N uptake, and subsequently a higher NH_4^+-N release (Figure 3.6c). However, it is also possible that the redox environment exceeded that of nitrate reduction, and is progressing through the redox profile of available electron acceptors, becoming more sulphidic.

4.4 Multifunctional observations

Combining nutrient species (NH_4^+-N, PO_4^{3-}-P and NO_x-N) in to one overall multifunctional measure (Figure 3.7) clearly shows that as eutrophication increased, the variability in function, particularly for sites 6 and 7 showed increased variability between chambers. Increased variability of this nature has been shown to indicate the onset of tipping point thresholds. This is where sudden and dramatic changes are seen, potentially moving the system to an alternative state (Hewitt & Thrush, 2019). Tipping points are not necessarily related to abrupt changes in a driver, but in the case of Waihī Estuary where nutrient and sediment inputs have been consistent for the previous 90 years, can also represent cumulative effects (Hewitt & Thrush, 2019). This is evident from the overlain vectors (Figure 3.7) showing that the increased variance between chambers at each site was explained by differences in OM, mud content, chl *a* and porosity.

4.5 Ecosystem level changes in function

Examination of the site by site differences in flux rates has reinforced that benthic intertidal habitats are a complex interconnected heterogeneous matrices of structure and function (Herman *et al.*, 1999; Lohrer *et al.*, 2004; Thrush *et al.*, 2012). Heterogeneity is a functionally important component of ecological systems (Thrush,

1991; Legendre, 1993; Archambault & Bourget, 1996) and in most cases results from non-random processes (Thrush *et al.*, 1999). Ecological processes operate over a continuum and across scales of both space and time (Hewitt *et al.*, 2007). Furthermore, local relationships (i.e. site level scale) may or may not reflect the broad scale relationships observed across the entire eutrophication gradient (Hewitt *et al.*, 2007).

To gain a more holistic understanding of the drivers of functioning at a system level, data from all sites along the gradient were integrated. By assimilating all seven sites in Multivariate Distance based Linear Models (DistLM), we can gain a better understanding of how small-scale processes influence change over an increasing spatial extent. In all cases, organic matter content was fitted first to the models, as by definition, eutrophication is the ecological response to the increased supply of OM content (Nixon, 1995). OM content in all models (with the exception of NO_x-N), significantly contributed towards explaining the variation and patterns in SOC, $GPP_{chl\ a}$, NH_4^+-N, and PO_4^{3-}-P.

OM content was highly positively correlated to mud %, reflecting movement from an advective (e.g., site 1) to a diffusion dominated (e.g., site 7) environment. It is important to note that solute exchange in both advective and diffusive environments benefit from the behaviours of sediment dwelling organisms (primarily bioturbation and bioirrigation). However, with increasing disturbance (OM and mud content increase) organism abundance and taxonomic richness declined. In Waihī Estuary, there were fewer bioturbators living in the diffusive sediments, further contributing to differences in solute fluxes. The following sections (4.5.1 to 4.5.3.3) relates to Table 3.9 and Table 3.10, and will discuss the physical and biological drivers that showed the greatest influence over this gradient.

4.5.1 Broad scale changes in dissolved oxygen

From less impacted to degraded environments in Waihī Estuary, a number of different factors contributed to the consumption of oxygen. In the less eutrophic environments, large fauna or fauna in high abundances can have significant influences in the drawdown of oxygen through respiration (Pelegri & Blackburn, 1994; Lohrer *et al.*, 2004; Sandwell *et al.*, 2009). DistLM results confirmed this by

the positive relationship between SOC (i.e., the demand of oxygen by the sediment) and *Paracorophium* spp., adult *M. liliana* and juvenile *M. liliana*. These results suggest that animals less tolerant to OM enrichment, particularly large *M. liliana* (that explained twice the variation of juvenile *M. liliana*) are respiring significant amounts of oxygen, creating a higher oxygen demand. This observation is most likely a function of biomass, as larger *M. liliana* respire more oxygen than the smaller biomass of juvenile *M. liliana*, and though *Paracorophium* spp. are small in size, they occurred in high densities. Middelburg and Levin (2009) review that aerobic respiration processes typically represent 25% of sediment oxygen consumption and that under a reduced environment a large portion of SOC in coastal sediments is attributable to re-oxidation processes.

SOC had a negative correlation with OM, and combined with chl *a*, explained the largest portion of the variance. As OM increased, particularly towards the more eutrophic end of the spectrum, chl *a* also increased which may indicate that excess OM derived from primary producers. The microphytes and algae that make up chl *a* will (in the dark) respire to consume oxygen, further contributing to SOC. Middelburg and Levin (2009) also indicate that as hypoxia increases along with the accumulation of OM, the OM that is buried is less degraded. This further shows that these hypoxic regions likely comprise labile chl *a* biomass, hence why phaeo (a degradation product of chl *a*) is not present in the DistLM model.

It would be expected that a positive relationship between OM and SOC would exist, however the negative relationship may be a reflection of the interactive effect of species loss from the system. Remineralisation of OM in the sediment increases the demand for oxygen, this can result in the mortality of macrofauna. As DO levels decrease (followed by macrofauna) a transition involving a number of geochemical and biological shifts alters the way oxygen is consumed (Rabalais *et al.*, 2014). Eutrophication can stimulate microbial oxygen consumption in the lower water column. Therefore, there is most likely an interaction between the respiration of macrofauna and microbial remineralisation.

As discussed in section 4.3.2.1, *Gracilaria* spp. can act as a cap over the sediment, reducing sediment oxygen exchange and impacting species abundance. Lewis and DeWitt (2017) showed that the cockle *Clinocardium nuttallii* mortality increased

by up to 50% in the presence of drifting algal mats which the cockles cannot evade through lateral movement. Sediment capped by algal mats may also lead to hypoxia, particularly during the warm summer months in which we sampled. Miyamoto *et al.* (2017) demonstrated that the effects of drifting algae on clam survival are temperature dependent, with warmer waters increasing the thickness and cover of the macroalgae.

4.5.2 **Broad scale changes in gross primary productivity**

The variation in $GPP_{chl\ a}$, a measure of photosynthetic efficiency, was explained almost equally by two variables; the first being a negative relationship with OM. Chl *a* represents a labile component of OM and is frequently used as a proxy for MPB biomass (Sandwell *et al.*, 2009; Jones, 2011). However, as OM enrichment in the system increases, the biomass of MPB can decrease (Pratt *et al.*, 2014b). Higher suspended sediment concentration (turbidity) in the water column is associated with an increase in fine sediments (correlated to OM), which can decrease light penetration to the bed (Kirk, 2010). Although eutrophic regions in Waihī Estuary had the highest chl *a* biomass, the chl *a* in these areas were less photosynthetically efficient at producing oxygen due to increased sediment input and reduced light penetration to the sediment bed. Pratt *et al.* (2014b) observed a three-fold reduction in NPP with increasing fine sediments; therefore reducing GPP and supporting the results of the current study.

Paracorophium spp. explained a large portion of the variance in $GPP_{chl\ a}$ and was negatively correlated. As demonstrated by our results and observations of Henriksen *et al.* (1983); Pelegri *et al.* (1994); Moraes *et al.* (2018), the high density and activity of *Paracorophium* spp. results in a significant bioturbational effect that can consume or promote the burial of MPB, therein reducing benthic primary production. With coarser grain sizes, the burial of MPB has less of an effect compared to finer grain sizes, as larger grains promote greater light attenuation though larger interstitial space (Kuhl *et al.*, 1994). *Paracorophium* spp. in our study were dominant in fine to medium sand sediments, although a relatively high proportion of mud was also present. A study by Moller and Riisgard (2006) found that in both laboratory and *in-situ* experiments, *Corophium volutator* changed

feeding behaviour from suspension feeding to surface deposit feeding when chl *a* concentrations were low; conditions similar to site 4.

4.5.3 **Broad scale changes in nutrients**

4.5.3.1 *Ammoniacal nitrogen*

Playing an important part in altering NH_4^+-N concentration across Waihi estuary were three variables explaining 89% of the variance overall. Physical variables, namely OM and phaeophytin, explained the largest portion of NH_4^+-N flux, followed by *A. stutchburyi*. In eutrophic, often oxygen deficient sediments NH_4^+-N is released due to less efficient nitrification pathways, i.e. less of the ammonium produced is re-oxidised (Middelburg & Levin, 2009). These findings are consistent with McCarthy *et al.* (2008) who found that DNRA was significantly higher in hypoxic sediments, furthering the release of NH_4^+-N by five to sevenfold through the absence of NH_4^+ cation exchange. Although a very different system to my study, Jäntti and Hietanen (2012) showed that DNRA dominates in anaerobic sediments of the Baltic Sea where nitrogen is not removed from the system, but instead is recycled; releasing, bioavailable NH_4^+-N and exacerbating the cycle of eutrophication.

Biological control of NH_4^+-N fluxes across the gradient was primarily driven by *A. stutchburyi* density. This relationship followed a negative trend, which was not observed at the site by site scale, and is opposite to the findings of Sandwell *et al.* (2009); Murphy *et al.* (2019). This highlights that, when examining the pattern across a gradient of change, interaction effects between both the sedimentary and biotic drivers should be considered. Increases in *A. stutchburyi* density and increased eutrophication both result in greater NH_4^+-N efflux. However, eutrophication simultaneously drives *A. stutchburyi* densities down whilst simultaneously enhancing NH_4^+-N efflux. Therefore, if the NH_4^+-N efflux, caused by increased eutrophication, outweighs the positive effect *A. stutchburyi* has on NH_4^+-N efflux, then the resultant relationship between NH_4^+-N and *A. stutchburyi* becomes negative. In the marginal tests, *A. stutchburyi* was not statistically significant, which may further indicate the aforementioned interactions are occurring.

4.5.3.2 *Phosphorus*

PO_4^{3-}-P was partially explained by a decrease in aRPD with increased eutrophication. Shallowing aRPD layers links to the loss of key bioturbators, whose activity plays an important role in mixing the surficial sediments and enhancing the sediment-water interface for oxidative exchange (Meysman *et al.*, 2006). Bioturbating fauna have been shown to increase the burial of organic phosphorus and Ca-P (Slomp *et al.*, 1996). However, our findings show a stimulation of PO_4^{3-}-P flux with increasing *A. stutchburyi* densities, which either points towards an un-sampled variable that may be affecting this relationship, or an interaction between variables that requires further study.

OM and phaeo explain a large portion of PO_4^{3-}-P variation and had the same positive relationship as NH_4^+-N. However, in this instance, phaeo explained a larger portion of the adjusted R^2 than OM (50 and 34% respectively). In oxic conditions PO_4^{3-}-P is bound to iron oxyhydroxides, but similarly with NH_4^+-N, as OM enrichment increases and hypoxia becomes more frequent, the bond between PO_4^{3-}-P and iron oxyhydroxides is reduced and PO_4^{3-}-P is rapidly released from the sediments (Algeo & Ingall, 2007; Hale *et al.*, 2016). Though we did not measure organic phosphorus (P), the burial of PO_4^{3-}-P generally occurs in the form of organic P or as calcium bound to phosphate (Ca-P) (Conley *et al.*, 2009a). The processes involved in the transformation of organic P in estuaries is poorly understood (Watson *et al.*, 2018). However, redox conditions influence the burial of organic P and Ca-P, as hypoxia decreases Ca-P formation and the burial of organic P (Conley *et al.*, 2009a). Therefore, an increase in the expansion of hypoxic areas may enhance the pool of easily mobilised PO_4^{3-}-P, setting up a positive feedback loop as eutrophic environments contribute to limited nutrient sequestration and greater phosphorus mobilisation (Watson *et al.*, 2018).

Another potentially contributing factor to PO_4^{3-}-P efflux are specific strains of heterotrophic and mixotrophic bacteria, for example, rapidly growing protozoa (Herman *et al.*, 1999), that exist in un-bioturbated sediments and excrete inorganic phosphorus at relatively high rates (Fenchel *et al.*, 2012). Due to the high surface area to volume ratio of finer grain sizes, bacterial biomass is also likely to be higher in eutrophic areas such as the upper reaches of Waihī Estuary. This warrants further study.

4.5.3.3 *Nitrite and nitrate*

There were three key drivers of NO_x-N, two sedimentary and one biological. The depth of oxygen penetration into the sediments (shown by aRPD) enhanced the efflux of NO_x-N, and chl *a* was also associated with an increase in NO_x-N. This is consistent with the site by site scale observations, where the pool of NO_x-N in anoxic sediments was likely either reduced to manganese or denitrified.

Ceratonereis spp. were shown to explain more variation in NO_x-N (accounting for the lower R^2 of NO_x-N) than *A. stutchburyi* explained for the solute fluxes. *Ceratonereis* spp. is a nereid polychaete that is classified as a deep dwelling, freely mobile scavenger that can be tolerant to a wide range of mud content (Greenfield *et al.*, 2016). This is consistent with the current study, where *Ceratonereis* spp. were found across all sites at varying densities. *Ceratonereis* spp. were negatively correlated with NO_x-N, which indicates that in sites where *Ceratonereis* spp. are less common, NO_x-N fluxes decrease. Nereid polychaetes have been well recognised as important bioturbators that can alter biogeochemical pathways, particularly the cycling of nitrogen (Welsh, 2003; Bosch *et al.*, 2015). A related species, *Ceratonereis aequisetis* has been shown to increase denitrification rates (De Roach *et al.*, 2002). Burrowing polychaetes are often associated with the drawdown of the water column solutes (Shull *et al.*, 2009; Quintana *et al.*, 2011). In the case of NO_x-N this can be nitrified and potentially quickly denitrified, as coupled nitrification-denitrification is often enhanced due to the strong oxic/anoxic boundaries along burrow walls (Kristensen *et al.*, 1991). Where larger NO_x-N influxes were seen, *Ceratonereis* spp. were also present in relatively high densities.

4.6 Implications for Waihī Estuary

If the primary stressors (i.e. sediment and nutrient loading, hypoxia) currently influencing Waihī Estuary continue to increase, further changes in ecosystem functioning are likely to occur. Increasing OM content was a major contributing factor to ecological shifts in this study. The increase in sediment oxygen demand associated with high OM loading indicates hypoxic (and potentially anoxic) conditions could expand, further altering system dynamics. In association with a reduction in dissolved oxygen flux, ammoniacal nitrogen release would elevate.

Dissolved reactive phosphorus follows this trend in reduced conditions. The influx of nitrite and nitrate into the sediment may increase with eutrophic stress to a point, and would also vary depending on the abundance of opportunistic species. Changes in community structure, reduced taxonomic richness and abundances as well as further loss of key species are likely to occur. This may impact the functional resilience of this system if the spatial extent and severity of eutrophication extends further down the gradient.

4.7 Future work

This study was a single comprehensive sampling effort performed in February 2018, during the height of New Zealand summer when light intensity, benthic primary productivity, and microbial and macrofaunal activities, were all likely at their annual peaks. Abiotic and biotic factors are known to vary seasonally, influencing the structure of the macrofaunal community and thereby ecosystem functions (Sundback *et al.*, 2000). Waihī Estuary is particularly dynamic and has floating algal blooms that are not present all year round. Having an experimental design that incorporates seasonal and multi-year trends in ecosystem function would further strengthen the study.

Sampling naturally occurring gradients encompasses all the stressors that occur with eutrophication. However, a lot of these stressors are highly correlated and interlinked. Further research to tease apart which stressor(s), (e.g. OM enrichment, sedimentation, hypoxia and pH), are most acute in driving changes in ecosystem function would enhance our understanding of eutrophic systems. This could be done by nesting manipulative studies within natural gradients (Hewitt *et al.*, 2007). Furthermore, some of the lesser studied bioturbators flagged as important in my study (e.g. *Paracorophium* spp. and *Ceratonereis* spp.) could be targeted in experiments that alter density and stress in order to better understand their contribution to ecosystem function.

My discussion also highlights the importance of the microbial realm, which is currently poorly understood; particularly the interactions between microbes and macrofauna. The work presented in this MSc (Research) thesis forms part of a wider project examining the microbial functioning of Waihī Estuary sediments.

Further analysis of bacterial functioning may explain some of the trends previously discussed. A more holistic view of the microbial processes may be established once denitrification fluxes and pore water nutrients (both collected from Waihī Estuary during this investigation) are analysed. This will add to our understanding of the nutrient dynamics, nitrogen losses and pathways in these sediments. Results from this study can provide a framework for other studies, as the effects of eutrophication are not limited to Waihī Estuary, but can be used to inform and evaluate the likely responses of other estuaries to eutrophication.

Chapter Five

Conclusion

I measured environmental variables, macrofaunal community structure and benthic solute fluxes at seven locations along a naturally occurring eutrophication gradient in Waihī Estuary. Biotic and abiotic drivers were analysed firstly on a site by site basis to gain resolution of fine scale dynamics. Non-metric distance based linear models were then employed to achieve the broader ecosystem scale of function across the spectrum of sites. The key findings of this study were:

- Benthic solute fluxes across Waihī Estuary varied spatially and in magnitude as a response of changes in the biological community structure to increased eutrophication and altered sediment conditions.

- Initial increases in eutrophication had non-linear effects on the macrofaunal community structure and abundance, where key large bioturbators were lost first (*Austrovenus stutchburyi* and *Macomona liliana*), followed by an increase in select opportunistic species (*Paracorophium* spp. and *Ceratonereis* spp.) that had disproportional effects on nutrient cycling.

- A shift in ecosystem functioning was seen at the upper reaches of Waihī Estuary (sites 6 and 7), where a three-fold increase in organic matter content coincided with a decrease in the macrofaunal taxonomic richness and abundance. This impacted ecosystem functioning by lowering dissolved oxygen concentrations, increasing NH_4^+-N and PO_4^{3-}-N efflux and greater NO_x-N influx.

While this study cannot make specific suggestions on how to manage Waihī Estuary, it is certainly evident that, in order to lessen the negative effects of eutrophication, mitigation strategies are required to protect the functioning of this estuary. Reducing terrestrial input of sediments and nutrients, as well as monitoring the downstream effects of these stressors would prevent further degradation and over time may restore function.

References

Adams, S. M. (2005). Assessing cause and effect of multiple stressors on marine systems. *Marine Pollution Bulletin, 51*(8-12), 649-657.

Algeo, T. J., & Ingall, E. (2007). Sedimentary C_{org} : P ratios, paleocean ventilation, and Phanerozoic atmospheric pO_2. *Palaeogeography, Palaeoclimatology, Palaeoecology, 256*(3-4), 130-155.

Anderson, D. M., Delaney, M. L., & Faul, K. L. (2001). Carbon to phosphorus ratios in sediments: Implications for nutrient cycling. *Global Biogeochemical Cycles, 15*(1), 65-79.

Anderson, M. J. (2008). Animal-sediment relationships re-visited: Characterising species' distributions along an environmental gradient using canonical analysis and quantile regression splines. *Journal of Experimental Marine Biology and Ecology, 366*(1-2), 16-27.

Anderson, M. J., Gorley, R. N., & Clarke, K. R. (2008). *PERMANOVA+ for PRIMER: Guide to software and statistical methods.* PRIMER-E Ltd, Plymouth, UK.

Arar, E., & Collins, G. (1997). *In vitro determination of chlorophyll a and pheophytin a in marine and freshwater algae by fluorescence.* U.S. Environmental Protection Agency, Cincinnati, Ohio.

Archambault, P., & Bourget, E. (1996). Scales of coastal heterogeneity and benthic intertidal species richness, diversity and abundance. *Marine Ecology Progress Series, 136*(1-3), 111-121.

Arndt, S., Jørgensen, B. B., LaRowe, D. E., Middelburg, J. J., Pancost, R. D., & Regnier, P. (2013). Quantifying the degradation of organic matter in marine sediments: A review and synthesis. *Earth-Science Reviews, 123*, 53-86.

Barbier, E. B. (2016). The protective value of estuarine and coastal ecosystem services in a wealth accounting framework. *Environmental & Resource Economics, 64*(1), 37-58.

Barbier, E. B., Hacker, S. D., Kennedy, C., Koch, E. W., Stier, A. C., & Silliman, B. R. (2011). The value of estuarine and coastal ecosystem services. *Ecological Monographs, 81*(2), 169-193.

Biles, C. L., Paterson, D. M., Ford, R. B., Solan, M., & Raffaelli, D. G. (2002). Bioturbation, ecosystem functioning and community structure. *Hydrology and Earth System Sciences, 6*(6), 999-1005.

Blackburn, T. H. (1986). Nitrogen-cycle in marine-sediments. *Ophelia, 26*, 65-76.

Blomqvist, S., Gunnars, A., & Elmgren, R. (2004). Why the limiting nutrient differs between temperate coastal seas and freshwater lakes: A matter of salt. *Limnology and Oceanography, 49*(6), 2236-2241.

Boesch, D. F. (2002). Challenges and opportunities for science in reducing nutrient over-enrichment of coastal ecosystems. *Estuaries, 25*(4), 886-900.

Bohorquez, J., Papaspyrou, S., Yufera, M., van Bergeijk, S. A., Garcia-Robledo, E., Jimenez-Arias, J. L., Bright, M., & Corzo, A. (2013). Effects of green macroalgal blooms on the meiofauna community structure in the Bay of Cadiz. *Marine Pollution Bulletin, 70*(1-2), 10-17.

Bosch, J. A., Cornwell, J. C., & Kemp, W. M. (2015). Short-term effects of nereid polychaete size and density on sediment inorganic nitrogen cycling under varying oxygen conditions. *Marine Ecology Progress Series, 524*, 155-169.

Botto, F., & Iribarne, O. (2000). Contrasting effects of two burrowing crabs (*Chasmagnathus granulata* and *Uca uruguayensis*) on sediment composition and transport in estuarine environments. *Estuarine, Coastal and Shelf Science, 51*(2), 141-151.

Boynton, W. R., Ceballos, M. A. C., Bailey, E. M., Hodgkins, C. L. S., Humphrey, J. L., & Testa, J. M. (2018). Oxygen and nutrient exchanges at the sediment-water interface: A global synthesis and critique of estuarine and coastal data. *Estuaries and Coasts, 41*(2), 301-333.

Bricker, S. B., Longstaf, B., Dennison, W., Jones, A., Boicourt, K., Wicks, C., & Woerner, J. (2008). Effects of nutrient enrichment in the nation's estuaries: A decade of change. *Harmful Algae, 8*(1), 21-32.

Burgin, A. J., & Hamilton, S. K. (2007). Have we overemphasized the role of denitrification in aquatic ecosystems? A review of nitrate removal pathways. *Frontiers in Ecology and the Environment, 5*(2), 89-96.

Canfield, D. E., Jørgensen, B. B., Fossing, H., Glud, R., Gundersen, J., Ramsing, N. B., Thamdrup, B., Hansen, J. W., Nielsen, L. P., & Hall, P. O. J. (1993). Pathways of organic-carbon oxidation in 3 continental-margin sediments. *Marine Geology, 113*(1-2), 27-40.

Cheung, S. G., & Shin, P. K. S. (2005). Size effects of suspended particles on gill damage in green-lipped mussel *Perna viridis*. *Marine Pollution Bulletin, 51*(8-12), 801-810.

Clarke, K. R., & Gorley, R. N. (2015). *PRIMER v7: User Manual/Tutorial*.

Cloern, J. E. (2001). Our evolving conceptual model of the coastal eutrophication problem. *Marine Ecology Progress Series, 210*, 223-253.

Conley, D. J. (1999). Biogeochemical nutrient cycles and nutrient management strategies. *Hydrobiologia, 410*, 87-96.

Conley, D. J., Bjorck, S., Bonsdorff, E., Carstensen, J., Destouni, G., Gustafsson, B. G., Hietanen, S., Kortekaas, M., Kuosa, H., Meier, H. E. M., Muller-Karulis, B., Nordberg, K., Norkko, A., Nurnberg, G., Pitkanen, H., Rabalais, N. N., Rosenberg, R., Savchuk, O. P., Slomp, C. P., Voss, M., Wulff, F., & Zillen, L. (2009a). Hypoxia-related processes in the Baltic Sea. *Environmental Science & Technology, 43*(10), 3412-3420.

Conley, D. J., Paerl, H. W., Howarth, R. W., Boesch, D. F., Seitzinger, S. P., Havens, K. E., Lancelot, C., & Likens, G. E. (2009b). Controlling eutrophication: Nitrogen and phosphorus. *Science, 323*(5917), 1014-1015.

Cosme, N., & Hauschild, M. Z. (2017). Characterization of waterborne nitrogen emissions for marine eutrophication modelling in life cycle impact assessment at the damage level and global scale. *International Journal of Life Cycle Assessment, 22*(10), 1558-1570.

Crawshaw, J. A., Schallenberg, M., & Savage, C. (2019). Physical and biological drivers of sediment oxygenation and denitrification in a New Zealand intermittently closed and open lake lagoon. *New Zealand Journal of Marine and Freshwater Research, 53*(1), 33-59.

Cummings, V. J., Pridmore, R. D., Thrush, S. F., & Hewitt, J. E. (1993). Emergence and floating behaviours of postsettlement juveniles of *Macomona liliana* (Bivalvia: Tellinacea). *Marine Behaviour and Physiology, 24*(1), 25-32.

Cummings, V. J., Pridmore, R. D., Thrush, S. F., & Hewitt, J. E. (1995). Postsettlement movement by intertidal benthic macroinvertebrates: Do common New Zealand species drift in the water column. *New Zealand Journal of Marine and Freshwater Research, 29*(1), 59-67.

Dalsgaard, T., Thamdrup, B., & Canfield, D. E. (2005). Anaerobic ammonium oxidation (anammox) in the marine environment. *Research in Microbiology, 156*(4), 457-464.

De Falco, G., Magni, P., Terasvuori, L. M. H., & Matteucci, G. (2004). Sediment grain size and organic carbon distribution in the Cabras Lagoon (Sardinia, Western Mediterranean). *Chemistry and Ecology, 20*, S367-S377.

De Roach, R. J., Rate, A. W., Knott, B., & Davies, P. M. (2002). Denitrification activity in sediment surrounding polychaete (*Ceratonereis aequisetis*) burrows. *Marine and Freshwater Research, 53*(1), 35-41.

Dean, H. K. (2008). The use of polychaetes (*Annelida*) as indicator species of marine pollution: A review. *Tropic Biological Journal, 56*, 11-38.

Delaney, M. L. (1998). Phosphorus accumulation in marine sediments and the oceanic phosphorus cycle. *Global Biogeochemical Cycles, 12*(4), 563-572.

Diaz, R. J., & Rosenberg, R. (2008). Spreading dead zones and consequences for marine ecosystems. *Science, 321*(5891), 926-929.

Douglas, E. J., Pilditch, C. A., Lohrer, A. M., Savage, C., Schipper, L. A., & Thrush, S. F. (2018). Sedimentary environment influences ecosystem response to nutrient enrichment. *Estuaries and Coasts, 41*(7), 1994-2008.

Drylie, T. P., Lohrer, A. M., Needham, H. R., Bulmer, R. H., & Pilditch, C. A. (2018). Benthic primary production in emerged intertidal habitats provides resilience to high water column turbidity. *Journal of Sea Research, 142*, 101-112.

Ellis, J. I., Hewitt, J. E., Clark, D., Taiapa, C., Patterson, M., Sinner, J., Hardy, D., & Thrush, S. F. (2015). Assessing ecological community health in coastal estuarine systems impacted by multiple stressors. *Journal of Experimental Marine Biology and Ecology, 473*, 176-187.

Emmerson, M. C., Solan, M., Emes, C., Paterson, D. M., & Raffaelli, D. (2001). Consistent patterns and the idiosyncratic effects of biodiversity in marine ecosystems. *Nature, 411*(6833), 73-77.

Falkowski, P. G., Barber, R. T., & Smetacek, V. (1998). Biogeochemical controls and feedbacks on ocean primary production. *Science, 281*(5374), 200-206.

Farrell, A. P., Richards, J. G., & Brauner, C. J. (2009). Defining hypoxia: An intergrative synthesis of the responses of fish to hypoxia. In J. G. Richards, A. P. Farrell & C. J. Brauner (Eds.), *Fish physiology: Hypoxia* (1 ed., Chapter 11, pp. 487-493). London, England: Elsevier.

Fenchel, T., Blackburn, H., King, G. M., & Blackburn, T. H. (2012). *Bacterial biogeochemistry: The ecophysiology of mineral cycling*. (3 ed.). China: Elsevier.

Fleeger, J. W., Carman, K. R., & Nisbet, R. M. (2003). Indirect effects of contaminants in aquatic ecosystems. *Science of the Total Environment, 317*(1-3), 207-233.

Froelich, P. N., Klinkhammer, G. P., Bender, M. L., Luedtke, N. A., Heath, G. R., Cullen, D., Dauphin, P., Hammond, D., Hartman, B., & Maynard, V. (1979). Early oxidation of organic-matter in pelagic sediments of the eastern equatorial atlantic - suboxic diagenesis. *Geochimica Et Cosmochimica Acta, 43*(7), 1075-1090.

Fuller, I. C., Macklin, M. G., & Richardson, J. M. (2015). The geography of the anthropocene in New Zealand: Differential river catchment response to human impact. *Geographical Research, 53*(3), 255-269.

Galloway, J. N., & Cowling, E. B. (2002). Reactive nitrogen and the world: 200 years of change. *Ambio, 31*(2), 64-71.

Galloway, J. N., Dentener, F. J., Capone, D. G., Boyer, E. W., Howarth, R. W., Seitzinger, S. P., Asner, G. P., Cleveland, C. C., Green, P. A., Holland, E. A., Karl, D. M., Michaels, A. F., Porter, J. H., Townsend, A. R., & Vorosmarty, C. J. (2004). Nitrogen cycles: Past, present, and future. *Biogeochemistry, 70*(2), 153-226.

Galloway, J. N., Townsend, A. R., Erisman, J. W., Bekunda, M., Cai, Z. C., Freney, J. R., Martinelli, L. A., Seitzinger, S. P., & Sutton, M. A. (2008). Transformation of the nitrogen cycle: Recent trends, questions, and potential solutions. *Science, 320*(5878), 889-892.

Glud, R. N. (2008). Oxygen dynamics of marine sediments. *Marine Biology Research, 4*(4), 243-289.

Gray, J. S., Wu, R. S. S., & Or, Y. Y. (2002). Effects of hypoxia and organic enrichment on the coastal marine environment. *Marine Ecology Progress Series, 238*, 249-279.

Green, M. O., & Coco, G. (2014). Review of wave-driven sediment resuspension and transport in estuaries. *Reviews of Geophysics, 52*(1), 77-117.

Greenfield, B. L., Kraan, C., Pilditch, C. A., & Thrush, S. F. (2016). Mapping functional groups can provide insight into ecosystem functioning and potential resilience of intertidal sandflats. *Marine Ecology Progress Series, 548*, 1-10.

Guillemin, M. L., Valero, M., Faugeron, S., Nelson, W., & Destombe, C. (2014). Tracing the Trans-Pacific evolutionary history of a domesticated seaweed (*Gracilaria chilensis*) with archaeological and genetic data. *Plos One, 9*(12), 17.

Hale, S. S., Cicchetti, G., & Deacutis, C. F. (2016). Eutrophication and hypoxia diminish ecosystem functions of benthic communities in a New England estuary. *Frontiers in Marine Science, 3*, 14.

Hattam, C., Atkins, J. P., Beaumont, N., Borger, T., Bohnke-Henrichs, A., Burdon, D., de Groot, R., Hoefnagel, E., Nunes, P., Piwowarczyk, J., Sastre, S., & Austen, M. C. (2015). Marine ecosystem services: Linking indicators to their classification. *Ecological Indicators, 49*, 61-75.

Heiri, O., Lotter, A. F., & Lemcke, G. (2001). Loss on ignition as a method for estimating organic and carbonate content in sediments: Reproducibility and comparability of results. *Journal of Paleolimnology, 25*(1), 101-110.

Henrichs, S. M., & Reeburgh, W. S. (1987). Anaerobic mineralization of marine sediment organic-matter: Rates and the role of anaerobic processes in the oceanic carbon economy. *Geomicrobiology Journal, 5*(3-4), 191-237.

Henriksen, K., & Kemp, W. M. (1988). Nitrification in estuarine and coastal marine sediments. In T. H. Blackburn & J. Sorensen (Eds.), *Nitrogen cycling in coastal marine environments*. Chichester, England: John Wiley & Sons Ltd.

Henriksen, K., Rasmussen, M. B., & Jensen, A. (1983). Effect of bioturbation on microbial nitrogen transformations in the sediment and fluxes of ammonium and nitrate to the overlaying water. *Ecological Bulletins* (35), 193-205.

Herbert, R. A. (1999). Nitrogen cycling in coastal marine ecosystems. *FEMS Microbiology Reviews, 23*(5), 563-590.

Herman, P. M. J., Middelburg, J. J., van de Koppel, J., & Heip, C. H. R. (1999). Ecology of estuarine macrobenthos. *Advances in Ecological Research, 29*, 195-240.

Hewitt, J. E., Legendre, P., McArdle, B. H., Thrush, S. F., Bellehumeur, C., & Lawrie, S. M. (1997). Identifying relationships between adult and juvenile bivalves at different spatial scales. *Journal of Experimental Marine Biology and Ecology, 216*(1-2), 77-98.

Hewitt, J. E., & Thrush, S. F. (2019). Monitoring for tipping points in the marine environment. *Journal of Environmental Management, 234*, 131-137.

Hewitt, J. E., Thrush, S. F., & Dayton, P. D. (2008). Habitat variation, species diversity and ecological functioning in a marine system. *Journal of Experimental Marine Biology and Ecology, 366*(1-2), 116-122.

Hewitt, J. E., Thrush, S. F., Dayton, P. K., & Bonsdorff, E. (2007). The effect of spatial and temporal heterogeneity on the design and analysis of empirical studies of scale-dependent systems. *American Naturalist, 169*(3), 398-408.

Huettel, M., & Gust, G. (1992). Impact of bioroughness on interfacial solute exchange in permeable sediments. *Marine Ecology Progress Series, 89*(2-3), 253-267.

Janssen, F., Huettel, M., & Witte, U. (2005). Pore-water advection and solute fluxes in permeable marine sediments (II): Benthic respiration at three sandy sites with different permeabilities (German Bight, North Sea). *Limnology and Oceanography, 50*(3), 779-792.

Jäntti, H., & Hietanen, S. (2012). The effects of hypoxia on sediment nitrogen cycling in the Baltic Sea. *Ambio, 41*(2), 161-169.

Jäntti, H., Stange, F., Leskinen, E., & Hietanen, S. (2011). Seasonal variation in nitrification and nitrate-reduction pathways in coastal sediments in the Gulf of Finland, Baltic Sea. *Aquatic Microbial Ecology, 63*(2), 171-181.

Jones, C. G., Lawton, J. H., & Shachak, M. (1994). Organsisms as ecosystem engineers. *Oikos, 69*(3), 373-386.

Jones, H. (2011). *The ecological role of the suspension feeding bivalve, Austrovenus stutchburyi, in estuarine ecosystems.* Doctoral thesis, University of Waikato, Hamilton.

Jørgensen, B. B. (1977a). Distribution of colorless sulfur bacteria (*Beggiatoa-spp.*) in a coastal marine sediment. *Marine Biology, 41*(1), 19-28.

Jørgensen, B. B. (1977b). Sulfur cycle of a coastal marine sediment (Limfjorden, Denmark). *Limnology and Oceanography, 22*(5), 814-832.

Jørgensen, B. B., & Revsbech, N. P. (1983). Colorless sulfur bacteria, *Beggiatoa spp*. and *Thiovulum spp*. in O_2 and H_2S microgradients. *Applied and Environmental Microbiology, 45*(4), 1261-1270.

Kamp, A., de Beer, D., Nitsch, J. L., Lavik, G., & Stief, P. (2011). Diatoms respire nitrate to survive dark and anoxic conditions. *Proceedings of the National Academy of Sciences of the United States of America, 108*(14), 5649-5654.

Karlson, K., Bonsdorff, E., & Rosenberg, R. (2007). The impact of benthic macrofauna for nutrient fluxes from Baltic Sea sediments. *Ambio, 36*(2-3), 161-167.

Kerner, M. (1993). Coupling of microbial fermentation and respiration processes in an intertidal mudflat of the Elbe Estuary. *Limnology and Oceanography, 38*(2), 314-330.

Kirk, J. T. O. (2010). *Light and photosynthesis in aquatic ecosystems* (3 ed.). Cambridge, New York: Cambridge University Press.

Kristensen, E. (1988). Benthic fauna and biogeochemical processes in marine sediments: Microbial activities and fluxes. In H. Blackburn & J. Sorensen (Eds.), *Nitrogen Cycling in Coastal Marine Environments* (pp. 275-300). John Wiley & Sons Ltd.

Kristensen, E. (2000). Organic matter diagenesis at the oxic/anoxic interface in coastal marine sediments, with emphasis on the role of burrowing animals. *Hydrobiologia, 426*(1-3), 1-24.

Kristensen, E., & Blackburn, T. H. (1987). The fate of organic-carbon and nitrogen in experimental marine sediment systems: Influence of bioturbation and anoxia. *Journal of Marine Research, 45*(1), 231-257.

Kristensen, E., Jensen, M. H., & Aller, R. C. (1991). Direct measurement of dissolved inorganic nitrogen exchange and denitrification in individual polychaete (*Nereis-virens*) burrows. *Journal of Marine Research, 49*(2), 355-377.

Kuhl, M., Lassen, C., & Jørgensen, B. B. (1994). Light penetration and light intensity in sandy marine sediments measured with irradiance and scalar irradiance fiber-optic microprobes. *Marine Ecology Progress Series, 105*, 139-148.

Legendre, P. (1993). Spatial autocorrelation: Trouble or new paradigm? *Ecology, 74*(6), 1659-1673.

Leica Microsystems. (2016). *Leica M50, Leica M60 & Leica M80 Stereomicroscopes: Technical Information.* Heerbrugg, Switzerland.

Levin, L. A., Ekau, W., Gooday, A. J., Jorissen, F., Middelburg, J. J., Naqvi, S. W. A., Neira, C., Rabalais, N. N., & Zhang, J. (2009). Effects of natural and human-induced hypoxia on coastal benthos. *Biogeosciences, 6*(10), 2063-2098.

Lewis, N. S., & DeWitt, T. H. (2017). Effect of green macroalgal blooms on the behavior, growth, and survival of cockles *Clinocardium nuttallii* in Pacific NW estuaries. *Marine Ecology Progress Series, 582*, 105-120.

Lohrer, A. M., Halliday, N. J., Thrush, S. F., Hewitt, J. E., & Rodil, I. F. (2010). Ecosystem functioning in a disturbance-recovery context: Contribution of macrofauna to primary production and nutrient release on intertidal sandflats. *Journal of Experimental Marine Biology and Ecology, 390*(1), 6-13.

Lohrer, A. M., Hewitt, J. E., Hailes, S. F., Thrush, S. F., Ahrens, M., & Halliday, J. (2011). Contamination on sandflats and the decoupling of linked ecological functions. *Austral Ecology, 36*(4), 378-388.

Lohrer, A. M., Rodil, I. F., Townsend, M., Chiaroni, L. D., Hewitt, J. E., & Thrush, S. F. (2013). Biogenic habitat transitions influence facilitation in a marine soft-sediment ecosystem. *Ecology, 94*(1), 136-145.

Lohrer, A. M., Thrush, S. F., & Gibbs, M. M. (2004). Bioturbators enhance ecosystem function through complex biogeochemical interactions. *Nature, 431*(7012), 1092-1095.

Lohrer, A. M., Townsend, M., Hailes, S. F., Rodil, I. F., Cartner, K., Pratt, D. R., & Hewitt, J. E. (2016). Influence of New Zealand cockles (*Austrovenus stutchburyi*) on primary productivity in sandflat-seagrass (*Zostera muelleri*) ecotones. *Estuarine, Coastal and Shelf Science, 181*, 238-248.

Lyons, D. A., Arvanitidis, C., Blight, A. J., Chatzinikolaou, E., Guy-Haim, T., Kotta, J., Orav-Kotta, H., Queiros, A. M., Rilov, G., Somerfield, P. J., & Crowe, T. P. (2014). Macroalgal blooms alter community structure and primary productivity in marine ecosystems. *Global Change Biology, 20*(9), 2712-2724.

Marsden, I. D., & Adkins, S. C. (2010). Current status of cockle bed restoration in New Zealand. *Aquaculture International, 18*(1), 83-97.

Marsden, I. D., & Bressington, M. J. (2009). Effects of macroalgal mats and hypoxia on burrowing depth of the New Zealand cockle (Austrovenus stutchburyi). *Estuarine Coastal and Shelf Science, 81*(3), 438-444.

McCartain, L. D., Townsend, M., Thrush, S. F., Wethey, D. S., Woodin, S. A., Volkenborn, N., & Pilditch, C. A. (2017). The effects of thin mud deposits on the behaviour of a deposit-feeding tellinid bivalve: Implications for ecosystem functioning. *Marine and Freshwater Behaviour and Physiology, 50*(4), 239-255.

McCarthy, M. J., McNeal, K. S., Morse, J. W., & Gardner, W. S. (2008). Bottom-water hypoxia effects on sediment-water interface nitrogen transformations in a seasonally hypoxic, shallow bay (Corpus Christi Bay, TX, USA). *Estuaries and Coasts, 31*(3), 521-531.

Meadows, P. S. (1964). Substrate selection by *Corophium* species: The particle size of substrates. *Journal of Animal Ecology, 33*(3), 387-394.

Meyer, S. T., Koch, C., & Weisser, W. W. (2015). Towards a standardized rapid ecosystem function assessment (REFA). *Trends in Ecology & Evolution, 30*(7), 390-397.

Meysman, F. J. R., Middelburg, J. J., & Heip, C. H. R. (2006). Bioturbation: A fresh look at Darwin's last idea. *Trends in Ecology & Evolution, 21*(12), 688-695.

Middelburg, J. J., & Levin, L. A. (2009). Coastal hypoxia and sediment biogeochemistry. *Biogeosciences, 6*(7), 1273-1293.

Miyamoto, Y., Yamada, K., Hatakeyama, K., & Hamaguchi, M. (2017). Temperature-dependent adverse effects of drifting macroalgae on the survival of Manila clams in a eutrophic coastal lagoon. *Plankton & Benthos Research, 12*(4), 238-247.

Moller, L. F., & Riisgard, H. U. (2006). Filter feeding in the burrowing amphipod *Corophium volutator*. *Marine Ecology Progress Series, 322*, 213-224.

Moraes, P. C., Zilius, M., Benelli, S., & Bartoli, M. (2018). Nitrification and denitrification in estuarine sediments with tube-dwelling benthic animals. *Hydrobiologia*, *819*(1), 217-230.

Murphy, A. E., Kolkmeyer, R., Song, B., Anderson, I. C., & Bowen, J. (2019). Bioreactivity and microbiome of biodeposits from filter-feeding bivalves. *Microbial Ecology*, *77*(2), 343-357.

Needham, H. R., Pilditch, C. A., Lohrer, A. M., & Thrush, S. F. (2010). Habitat dependence in the functional traits of *Austrohelice crassa*, a key bioturbating species. *Marine Ecology Progress Series, 414*, 179-193.

Needham, H. R., Pilditch, C. A., Lohrer, A. M., & Thrush, S. F. (2011). Context-specific bioturbation mediates changes to ecosystem functioning. *Ecosystems, 14*(7), 1096-1109.

Nelson, W. A., Neill, K. F., & D'Archino, R. (2015). When seaweeds go bad: An overview of outbreaks of nuisance quantities of marine macroalgae in New Zealand. *New Zealand Journal of Marine and Freshwater Research, 49*(4), 472-491.

Nixon, S. W. (1995). Coastal marine eutrophication: A definition, social causes, and future concerns. *Ophelia, 41*(1), 199-219.

Nixon, S. W., Ammerman, J. W., Atkinson, L. P., Berounsky, V. M., Billen, G., Boicourt, W. C., Boynton, W. R., Church, T. M., Ditoro, D. M., Elmgren, R., Garber, J. H., Giblin, A. E., Jahnke, R. A., Owens, N. J. P., Pilson, M. E. Q., & Seitzinger, S. P. (1996). The fate of nitrogen and phosphorus at the land sea margin of the North Atlantic Ocean. *Biogeochemistry, 35*(1), 141-180.

Norkko, A., Thrush, S. F., Hewitt, J. E., Cummings, V. J., Norkko, J., Ellis, J. I., Funnell, G. A., Schultz, D., & MacDonald, I. (2002). Smothering of estuarine sandflats by terrigenous clay: The role of wind-wave disturbance and bioturbation in site-dependent macrofaunal recovery. *Marine Ecology Progress Series, 234*, 23-41.

Norkko, A., Villnas, A., Norkko, J., Valanko, S., & Pilditch, C. (2013). Size matters: Implications of the loss of large individuals for ecosystem function. *Scientific Reports, 3*, 1-7.

Norkko, J., Hewitt, J. E., & Thrush, S. F. (2006). Effects of increased sedimentation on the physiology of two estuarine soft-sediment bivalves, *Austrovenus stutchburyi* and *Paphies australis*. *Journal of Experimental Marine Biology and Ecology, 333*(1), 12-26.

O'Meara, T. A., Hillman, J. R., & Thrush, S. F. (2017). Rising tides, cumulative impacts and cascading changes to estuarine ecosystem functions. *Scientific Reports, 7*, 7.

ONSET. (2018). *HOBO®UA-002-64 Data Logger.* Bourne, MA.

Paerl, H. W. (2006). Assessing and managing nutrient-enhanced eutrophication in estuarine and coastal waters: Interactive effects of human and climatic perturbations. *Ecological Engineering, 26*(1), 40-54.

Park, S. (2016). *Ecological health of Waihī Estuary.* Bay of Plenty Regional Council, New Zealand.

Paytan, A., & McLaughlin, K. (2007). The oceanic phosphorus cycle. *Chemical Reviews, 107*(2), 563-576.

Pearson, T. H., & Rosenberg, R. (1978). Macrobenthic succession in relation to organic enrichment and pollution of the marine environment. *Oceanography Marine Biology, 16*, 229-311.

Pelegri, S. P., & Blackburn, T. H. (1994). Bioturbation effects of the amphipod *Corophium volutator* on microbial nitrogen transformations in marine-sediments. *Marine Biology, 121*(2), 253-258.

Pelegri, S. P., Nielsen, L. P., & Blackburn, T. H. (1994). Denitrification in estuarine sediment stimulated by the irrigation activity of the amphipod *Corophium volutator*. *Marine Ecology Progress Series, 105*(3), 285-290.

Peters, R. H. (1983). *The ecological implications of body size*. (Vol. 2). Cambridge; NY: Cambridge University Press.

Potter, I. C., Chuwen, B. M., Hoeksema, S. D., & Elliott, M. (2010). The concept of an estuary: A definition that incorporates systems which can become closed to the ocean and hypersaline. *Estuarine Coastal and Shelf Science, 87*(3), 497-500.

Pratt, D. R., Lohrer, A. M., Pilditch, C. A., & Thrush, S. F. (2014a). Changes in ecosystem function across sedimentary gradients in estuaries. *Ecosystems, 17*(1), 182-194.

Pratt, D. R., Pilditch, C. A., Lohrer, A. M., & Thrush, S. F. (2014b). The effects of short-term increases in turbidity on sandflat microphytobenthic productivity and nutrient fluxes. *Journal of Sea Research, 92*, 170-177.

Precision Measurement Engineering. (2014). *miniDO$_2$T User's Manual.* Vista, CA.

PreSens. (2009). *Fibox 3 LCD trace v7.* Regensburg, Germany.

Quintana, C. O., Hansen, T., Delefosse, M., Banta, G., & Kristensen, E. (2011). Burrow ventilation and associated porewater irrigation by the polychaete *Marenzelleria viridis*. *Journal of Experimental Marine Biology and Ecology, 397*(2), 179-187.

Rabalais, N. N., Cai, W. J., Carstensen, J., Conley, D. J., Fry, B., Hu, X. P., Quinones-Rivera, Z., Rosenberg, R., Slomp, C. P., Turner, R. E., Voss, M., Wissel, B., & Zhang, J. (2014). Eutrophication-driven deoxygenation in the coastal ocean. *Oceanography, 27*(1), 172-183.

Rabalais, N. N., Diaz, R. J., Levin, L. A., Turner, R. E., Gilbert, D., & Zhang, J. (2010). Dynamics and distribution of natural and human-caused hypoxia. *Biogeosciences, 7*(2), 585-619.

Rabalais, N. N., Turner, R. E., Diaz, R. J., & Justic, D. (2009). Global change and eutrophication of coastal waters. *Ices Journal of Marine Science, 66*(7), 1528-1537.

Ruttenberg, K. C. (2014). *The global phosphorus cycle*. Treatise on Geochemistry (2 ed., Vol. 10). Oxford, England: Elsevier.

Rysgaard, S., Risgaardpetersen, N., Sloth, N. P., Jensen, K., & Nielsen, L. P. (1994). Oxygen regulation of nitrification and denitrification in sediments. *Limnology and Oceanography, 39*(7), 1643-1652.

Sandwell, D. R., Pilditch, C. A., & Lohrer, A. M. (2009). Density dependent effects of an infaunal suspension-feeding bivalve (*Austrovenus stutchburyi*) on sandflat nutrient fluxes and microphytobenthic productivity. *Journal of Experimental Marine Biology and Ecology, 373*(1), 16-25.

Scholes, P. (2015). *NERMN estuary water quality report 2014.* Whakatane, New Zealand. Bay of Plenty Regional Council.

Shannon, C. E. (1948). A mathematical theory of communication. *The Bell System Technical Journal, 27*(3), 379-423.

Shull, D. H., Benoit, J. M., Wojcik, C., & Senning, J. R. (2009). Infaunal burrow ventilation and pore-water transport in muddy sediments. *Estuarine Coastal and Shelf Science, 83*(3), 277-286.

Sigman, D. M., & Hain, M. P. (2012). The biological productivity of the ocean. *Nature Education Knowledge, 3*(6), 1-16.

Singer, J. K., Anderson, J. B., Ledbetter, M. T., McCave, I. N., Jones, K. P. N., & Wright, R. (1988). An assessment of analytical techniques for the size analysis of fine-grained sediments. *Journal of Sedimentary Petrology, 58*(3), 534-543.

Slomp, C. P., Epping, E. H. G., Helder, W., & Van Raaphorst, W. (1996). A key role for iron-bound phosphorus in authigenic apatite formation in North Atlantic continental platform sediments. *Journal of Marine Research, 54*(6), 1179-1205.

Sørensen, J. J., B. B., & Revsbech, N. P. (1979). A comparison of oxygen, nitrate, and sulfate respiration in coastal marine sediments. *Microbial Ecology, 5*(2), 105-115.

Spinelli, G. A., Giambalvo, E. R., & Fisher, A. T. (2004). Sediment permeability, distribution, and influence on fluxes in oceanic basement. In E. E. Davis & H. Elderfield (Eds.), *Hydrogeology of the Oceanic Lithosphere* (Chapter 6, pp. 151-188). Cambridge, England: Cambridge University Press.

Stief, P. (2013). Stimulation of microbial nitrogen cycling in aquatic ecosystems by benthic macrofauna: Mechanisms and environmental implications. *Biogeosciences, 10*(12), 7829-7846.

Sundback, K., Miles, A., & Goransson, E. (2000). Nitrogen fluxes, denitrification and the role of microphytobenthos in microtidal shallow-water sediments: An annual study. *Marine Ecology Progress Series, 200*, 59-76.

Sundby, B., Gobeil, C., Silverberg, N., & Mucci, A. (1992). The phosphorus cycle in coastal marine-sediments. *Limnology and Oceanography, 37*(6), 1129-1145.

Suren, A., Park, A., Carter, R., Fernandes, R., Bloor, M., Barber, J., & Dean, S. (2016). *Kaituna-Maketū and Pongakawa-Waitahanui water management area: Current state and gap analysis.* Whakatane, New Zealand. Bay of Plenty Regional Council.

Tay, H. W., Bryan, K. R., & Pilditch, C. A. (2013). Dissolved inorganic nitrogen concentrations in an estuarine tidal flat. *Journal of Coastal Research*(65), 135-140.

Teixeira, C., Magalhaes, C., Boaventura, R. A. R., & Bordalo, A. A. (2010). Potential rates and environmental controls of denitrification and nitrous oxide production in a temperate urbanized estuary. *Marine Environmental Research, 70*(5), 336-342.

Tengberg, A., Stahl, H., Gust, G., Muller, V., Arning, U., Andersson, H., & Hall, P. O. J. (2004). Intercalibration of benthic flux chambers I. Accuracy of flux measurements and influence of chamber hydrodynamics. *Progress in Oceanography, 60*(1), 1-28.

Thrush, S. F. (1991). Spatial patterns in soft-bottom communities. *Trends in Ecology & Evolution, 6*(3), 75-79.

Thrush, S. F., Hewitt, J. E., Cummings, V., Ellis, J. I., Hatton, C., Lohrer, A., & Norkko, A. (2004). Muddy waters: Elevating sediment input to coastal and estuarine habitats. *Frontiers in Ecology and the Environment, 2*(6), 299-306.

Thrush, S. F., Hewitt, J. E., Gibbs, M., Lundquist, C., & Norkko, A. (2006). Functional role of large organisms in intertidal communities: Community effects and ecosystem function. *Ecosystems, 9*(6), 1029-1040.

Thrush, S. F., Hewitt, J. E., Hickey, C. W., & Kelly, S. (2008). Multiple stressor effects identified from species abundance distributions: Interactions between urban contaminants and species habitat relationships. *Journal of Experimental Marine Biology and Ecology, 366*(1-2), 160-168.

Thrush, S. F., Hewitt, J. E., Kraan, C., Lohrer, A. M., Pilditch, C. A., & Douglas, E. (2017). Changes in the location of biodiversity - ecosystem function hot spots across the seafloor landscape with increasing sediment nutrient loading. *Proceedings of the Royal Society B: Biological Sciences, 284*(1852), 10.

Thrush, S. F., Hewitt, J. E., & Lohrer, A. M. (2012). Interaction networks in coastal soft-sediments highlight the potential for change in ecological resilience. *Ecological Applications, 22*(4), 1213-1223.

Thrush, S. F., Lawrie, S. M., Hewitt, J. E., & Cummings, V. J. (1999). *The problem of scale: Uncertainties and implications for soft-bottom marine communities and the assessment of human impacts*. Biogeochemical Cycling and Sediment Ecology (Vol. 59). Dordrecht, Netherlands: Springer.

TIBCO Software Inc. (2018). *Statistica (data analysis software system).*

Trimble Inc. (2019). *SketchUp version 1.2* [Computer program]. https://www.sketchup.com.

Tsutsumi, H. (1990). Population persistence of *Capitella sp* (Polychaeta; Capitellidae) on a mud flat subject to environmental disturbance by organic enrichment. *Marine Ecology Progress Series, 63*(2-3), 147-156.

Underwood, G. J. C., & Kromkamp, J. (1999). Primary production by phytoplankton and microphytobenthos in estuaries. In D. B. Nedwell & D. G. Raffaelli (Eds.), *Advances in Ecological Research, Vol 29: Estuaries* (pp. 93-153). San Diego: Elsevier Academic Press Inc.

Valiela, I., Bartholomew, M., Giblin, A., Tucker, J., Harris, C., Martinetto, P., Otter, M., Camilli, L., & Stone, T. (2014). Watershed deforestation and down-estuary transformations alter sources, transport, and export of suspended particles in Panamanian mangrove estuaries. *Ecosystems, 17*(1), 96-111.

Vaquer-Sunyer, R., & Duarte, C. M. (2008). Thresholds of hypoxia for marine biodiversity. *Proceedings of the National Academy of Sciences of the United States of America, 105*(40), 15452-15457.

Vitousek, P. M., Aber, J. D., Howarth, R. W., Likens, G. E., Matson, P. A., Schindler, D. W., Schlesinger, W. H., & Tilman, D. (1997). Human alteration of the global nitrogen cycle: Sources and consequences. *Ecological Applications, 7*(3), 737-750.

Watson, S. J., Cade-Menun, B. J., Needoba, J. A., & Peterson, T. D. (2018). Phosphorus forms in sediments of a river-dominated estuary. *Frontiers in Marine Science, 5*, 11.

Webb, A. P., & Eyre, B. D. (2004). The effect of natural populations of the burrowing and grazing soldier crab (*Mictyris longicarpus*) on sediment irrigation, benthic metabolism and nitrogen fluxes. *Journal of Experimental Marine Biology and Ecology, 309*(1), 1-19.

Wellnitz, T., & Poff, N. L. (2001). Functional redundancy in heterogeneous environments: Implications for conservation. *Ecology Letters, 4*(3), 177-179.

Welsh, D. T. (2003). It's a dirty job but someone has to do it: The role of marine benthic macrofauna in organic matter turnover and nutrient recycling to the water column. *Chemistry and Ecology, 19*(5), 321-342.

Wentworth, C. K. (1922). A scale of grade and class terms for clastic sediments. *The Journal of Geology, 30*(5), 377-392.

Woodward, F. I. (1994). How many species are required for a functional ecosystem? In E. D. Schulze & H. A. Mooney (Eds.), *Biodiversity and ecosystem function* (pp. 271-291). Berlin, Heidelberg: Springer.

Appendices

Appendix 1

Table A.1: SIMPER analysis (Bray-Curtis similarity) of square-root transformed macrofauna data comparing all other SIMPER analyses of sites not included in section 3.2. Percentage dissimilarity between sites and a listing of the species collectively contributing to 50% of the dissimilarity between specific pairs of sites. Average abundance of the key species, their percent contribution to cumulative dissimilarity, and the dissimilarity to standard deviation ratio (Diss/SD) are also given.

Sites	Species	Site dis-similarity (%)	Average N		Species dis-similarity (%)	Contribution (%)	Diss/SD
1 & 2		**52.61**	**Site 1**	**Site 2**			
	Austrovenus stutchburyi		9.32	1.90	8.08	15.37	6.72
	Prionospio aucklandica		5.03	0.10	5.37	10.21	6.50
	Colurostylis lemurum		0.20	4.80	4.93	9.37	1.86
	Paphies australis		0.47	3.46	3.35	6.37	1.77
	Ceratonereis spp.		5.90	3.19	2.97	5.65	2.88
	Austrominius modestus		2.91	0.51	2.71	5.15	1.42
1 & 6		**75.78**	**Site 1**	**Site 6**			
	Austrovenus stutchburyi		9.32	0.10	11.63	15.35	7.88
	Paracorophium spp.		0.1	8.01	9.89	13.05	6.75
	Prionospio aucklandica		5.03	0.10	6.21	8.20	6.11
	Macomona liliana		3.95	0.00	4.97	6.56	6.44
	Anthritica bifurca		0.00	3.91	4.85	6.40	3.65
	Austrominius modestus		2.91	0.00	3.62	4.78	1.71
2 & 3		**68.75**	**Site 2**	**Site 3**			
	Prionospio aucklandica		0.10	11.27	13.23	19.24	7.32
	Colurostylis lemurum		4.80	0.00	5.60	8.15	1.99
	Microspio maori		3.81	0.20	4.28	6.22	5.22
	Paphies australis		3.46	0.00	4.08	5.94	1.92
	Anthropleura aureoradiata		1.06	4.48	3.95	5.75	1.95
	Austrovenus stutchburyi		1.90	5.03	3.70	5.38	3.17
2 & 4		**72.14**	**Site 2**	**Site 4**			
	Paracorophium spp.		1.34	15.24	18.35	25.44	3.72
	Colurostylis lemurum		4.80	0.10	6.10	8.45	1.94
	Microspio maori		3.81	0.17	4.85	6.72	4.14
	Paphies australis		3.46	0.00	4.54	6.30	1.91
	Edwardsia		2.73	0.00	3.59	4.98	3.42
2 & 5		**71.92**	Site 2	Site 5			
	Paracorophium spp.		1.34	7.63	10.39	14.45	2.20
	Colurostylis lemurum		4.80	0.00	7.62	10.60	2.03
	Microspio maori		3.81	0.00	6.22	8.65	5.33
	Paphies australis		3.46	0.00	5.58	7.76	1.88

	Edwardsia		2.73	0.00	4.41	6.14	3.37
	Oligochaeta		3.97	2.08	3.75	5.21	1.30
2 & 6		**73.01**	**Site 2**	**Site 6**			
	Paracorophium spp.		1.34	8.01	9.93	13.6	3.22
	Colurostylis lemurum		4.80	0.00	6.96	9.54	2.01
	Anthritica bifurca		0.10	3.91	5.57	7.63	3.39
	Paphies australis		3.46	0.00	5.09	6.97	1.89
	Microspio maori		3.81	1.10	4.05	5.55	3.26
	Edwardsia		2.73	0.00	4.02	5.51	3.39
	Macomona liliana		2.60	0.00	3.86	5.28	6.10
2 & 7		**85.83**	**Site 2**	**Site 7**			
	Colurostylis lemurum		4.80	0.00	10.15	11.83	2.13
	Microspio maori		3.81	0.00	8.38	9.76	5.41
	Paphies australis		3.46	0.00	7.47	8.70	1.87
	Oligochaeta		3.97	2.39	6.00	6.99	1.64
	Edwardsia		2.73	0.00	5.92	6.89	3.51
	Macomona liliana		2.60	0.10	5.47	6.38	4.91
3 & 4		**66.50**	**Site 3**	**Site 4**			
	Paracorophium spp.		0.00	15.24	18.96	28.51	4.76
	Prionospio aucklandica		11.27	2.78	10.55	15.86	4.73
	Anthropleura aureoradiata		4.48	0.20	5.25	7.89	2.49
	Austrovenus stutchburyi		5.03	2.48	3.19	4.8	2.78
3 & 5		**81.92**	**Site 3**	**Site 5**			
	Prionospio aucklandica		11.27	0.57	16.21	19.79	5.72
	Paracorophium spp.		0.00	7.63	11.58	14.14	3.15
	Anthropleura aureoradiata		4.48	0.00	6.63	8.09	2.79
	Austrovenus stutchburyi		5.03	0.91	6.25	7.63	4.49
	Aonides trifida		3.44	0.00	5.22	6.37	3.46
3 & 6		**80.76**	**Site 3**	**Site 6**			
	Prionospio aucklandica		11.27	0.10	15.5	19.19	6.94
	Paracorophium spp.		0.00	8.01	11.09	13.73	6.7
	Austrovenus stutchburyi		5.03	0.1	6.88	8.52	5.73
	Anthropleura aureoradiata		4.48	0.00	6.09	7.54	2.76
	Macomona liliana		3.77	0.00	5.27	6.52	5.14
3 & 7		**91.68**	**Site 3**	**Site 7**			
	Prionospio aucklandica		11.27	0.00	22.35	24.38	9.02
	Austrovenus stutchburyi		5.03	0.20	9.66	10.54	5.55
	Anthropleura aureoradiata		4.48	0.10	8.44	9.21	2.86
	Macomona liliana		3.77	0.10	7.37	8.04	4.57
4 & 5		**50.20**	**Site 4**	**Site 5**			
	Paracorophium spp.		15.24	7.63	13.30	26.49	1.91
	Macomona liliana		3.55	0.40	5.58	11.11	3.13
	Capitella		0.10	2.82	4.71	9.39	2.63
	Prionospio aucklandica		2.78	0.57	4.00	7.96	1.79
4 & 6		**52.90**	**Site 4**	**Site 6**			
	Paracorophium spp.		15.24	8.01	11.36	21.47	1.89
	Macomona liliana		3.55	0.00	5.68	10.74	3.94
	Prionospio aucklandica		2.78	0.10	4.29	8.10	2.52

	Ceratonereis spp.		1.53	3.93	3.81	7.20	1.91
	Austrovenus stutchburyi		2.48	0.10	3.80	7.18	3.18
4 & 7		**88.85**	**Site 4**	**Site 7**			
	Paracorophium spp.		15.24	0.34	35.51	39.97	5.33
	Macomona liliana		3.55	0.10	8.48	9.55	3.37
	Scolecolepides benhami		2.98	0.00	7.19	8.09	4.90
5 & 6		**47.04**	**Site 5**	**Site 6**			
	Anthritica bifurca		0.71	3.91	6.57	13.96	2.12
	Ceratonereis spp.		1.39	3.93	5.02	10.66	2.04
	Paracorophium spp.		7.63	8.01	4.73	10.07	1.46
	Capitella		2.82	0.90	3.92	8.34	1.79
	Oligochaeta		2.08	2.13	3.19	6.78	1.24
	Nicon aestuariensis		0.30	1.60	2.71	5.77	2.01
5 & 7		**83.29**	**Site 5**	**Site 7**			
	Paracorophium spp.		7.63	0.34	26.86	32.25	2.97
	Capitella		2.82	0.00	10.12	12.15	3.29
	Oligochaeta		2.08	2.39	7.88	9.46	1.15
6 & 7		**81.12**	**Site 6**	**Site 7**			
	Paracorophium spp.		8.01	0.34	22.83	28.14	6.20
	Anthritica bifurca		3.91	0.00	11.44	14.10	4.55
	Ceratonereis spp.		3.93	0.89	8.89	10.96	2.62

Appendix 2

Table A.2: DistLM marginal tests for response variables not included in sequential tests of SOC, $GPP_{chl\ a}$, dark chamber NH_4^+-N, dark chamber PO_4^{3-}-P and dark chamber NO_x-N in section 3.5.1. OM: *organic matter content, chl a: chlorophyll a, phaeo: phaeophytin, aRPD: apparent redox discontinuity potential, Por: porosity, SOC: sediment oxygen consumption, $GPP_{Chl\ a}$: gross primary productivity normalised by chlorophyll a,* NH_4^+-N*: ammonium,* PO_4^{3-}-P*: dissolved reactive phosphorus,* NO_x-N*: nitrate-nitrite nitrogen.*

	Variable	SS(trace)	Pseudo-F	P	Prop.
DO					
	Med GS	2.20	2.28	0.14	0.07
	Mud %	7.54	9.56	<0.01	0.24
	Por	6.41	7.76	0.01	0.20
	Phaeo (µg/g)	13.09	21.47	<0.01	0.41
	aRPD	13.11	21.50	<0.01	0.41
	SW	0.84	0.83	0.36	0.03
	N	3.46	3.75	0.04	0.11
	S	5.37	6.25	0.02	0.17
	A. stutchburyi <10 mm	0.49	0.48	0.47	0.02
	A. stutchburyi >10 mm	<0.01	<0.01	0.97	<0.01
	Total *A. stutchburyi*	0.49	0.48	0.50	0.02
	Total *M. liliana*	0.19	0.19	0.69	0.01
	Paracorophium spp.	8.06	10.44	<0.01	0.25
	Ceratonereis spp.	0.45	0.44	0.53	0.01
$GPP_{chl\ a}$					
	Med GS	14.64	26.15	<0.01	0.46
	Mud %	11.32	16.97	<0.01	0.35
	P	8.03	10.39	0.01	0.25
	Chl a (µg/g)	12.31	19.38	<0.01	0.38
	Phaeo (µg/g)	3.18	3.42	0.09	0.10
	Gracilaria spp.	4.11	4.57	0.04	0.13
	aRPD	0.28	0.27	0.60	0.01
	SW	7.76	9.92	0.01	0.24
	N	0.07	0.07	0.78	<0.01
	S	6.10	7.30	0.01	0.19
	A. stutchburyi <10 mm	3.25	3.50	0.07	0.10
	A. stutchburyi >10 mm	0.02	0.01	0.91	<0.01
	M. liliana <10 mm	0.37	0.36	0.56	0.01
	M. liliana >10 mm	9.76	13.61	<0.01	0.31
	Total *A. stutchburyi*	3.25	3.51	0.08	0.10
	Total *M. liliana*	3.68	4.02	0.05	0.11
	Ceratonereis spp.	0.85	0.84	0.37	0.03
NH_4^+-N					
	Med GS	17.01	35.18	<0.01	0.53

	Mud %	20.70	56.77	<0.01	0.65
	P	17.38	36.84	<0.01	0.54
	Chl a (µg/g)	7.41	9.35	0.01	0.23
	Gracilaria spp.	24.80	106.84	<0.01	0.78
	aRPD	15.84	30.40	<0.01	0.50
	SW	2.82	3.00	0.11	0.09
	N	4.15	4.61	0.03	0.13
	S	9.34	12.78	<0.01	0.29
	A. stutchburyi <10 mm	<0.01	<0.01	1.00	<0.01
	A. stutchburyi >10 mm	2.42	2.53	0.11	0.08
	M. liliana <10 mm	0.92	0.91	0.34	0.03
	M. liliana >10 mm	1.50	1.52	0.25	0.05
	Total *M. liliana*	1.66	1.69	0.20	0.05
	Ceratonereis spp.	0.13	0.13	0.73	<0.01
PO_4^{3-}-P					
	Med GS	5.16	5.95	0.02	0.16
	Mud %	6.28	7.58	0.01	0.20
	P	4.08	4.53	0.06	0.13
	Chl a (µg/g)	0.87	0.87	0.37	0.03
	Gracilaria spp.	14.15	24.56	<0.01	0.44
	SW	5.68	6.69	0.01	0.18
	N	<0.01	<0.01	0.99	<0.01
	S	4.69	5.33	0.02	0.15
	A. stutchburyi <10 mm	0.07	0.07	0.78	<0.01
	A. stutchburyi >10 mm	<0.01	<0.01	0.96	<0.01
	M. liliana <10 mm	0.57	0.57	0.45	0.02
	M. liliana >10 mm	0.48	0.47	0.52	0.02
	Total *M. liliana*	0.06	0.06	0.81	<0.01
	Paracorophium spp.	0.05	0.05	0.81	<0.01
	Ceratonereis spp.	0.96	0.96	0.31	0.03
NO_x-N					
	Med GS	0.68	0.67	0.42	0.02
	Mud %	0.34	0.33	0.55	0.01
	P	0.17	0.17	0.69	0.01
	Phaeo (µg/g)	0.57	0.56	0.46	0.02
	Gracilaria spp.	0.42	0.42	0.51	0.01
	SW	0.74	0.74	0.40	0.02
	N	2.35	2.46	0.13	0.07
	S	0.01	0.01	0.91	<0.01
	A. stutchburyi <10 mm	0.16	0.15	0.72	<0.01
	A. stutchburyi >10 mm	3.04	3.25	0.08	0.09
	M. liliana <10 mm	3.52	3.83	0.06	0.11
	M. liliana >10 mm	0.47	0.46	0.49	0.01
	Total *A. stutchburyi*	0.22	0.22	0.66	0.01
	Total *M. liliana*	2.96	3.16	0.09	0.09
	Paracorophium spp.	1.57	1.60	0.20	0.05